Desert Research Institute

University and Community College System of Nevada

# Measurements and Validation for the Twelve Month Particulate Matter Study in Hong Kong

Final Report


PREPARED BY:

Dr. Judith C. Chow
Dr. John G. Watson
Mr. Steven D. Kohl
Mr. Hal E. Voepel
Dr. L.-W. Antony Chen

DESERT RESEARCH INSTITUTE
2215 Raggio Parkway
Reno, NV 89512
USA


PREPARED FOR:

Environmental Protection Department
The Government of Hong Kong Special Administrative Region
33/F, Revenue Tower
5 Gloucester Rd.
Wan Chai
Hong Kong

July 12, 2006

# Measurements and Validation for the Twelve Month Particulate Matter Study in Hong Kong

Final Report


PREPARED BY:

Dr. Judith C. Chow
Dr. John G. Watson
Mr. Steven D. Kohl
Mr. Hal E. Voepel
Dr. L.-W. Antony Chen

DESERT RESEARCH INSTITUTE
2215 Raggio Parkway
Reno, NV 89512
USA


PREPARED FOR:

Environmental Protection Department
The Government of Hong Kong Special Administrative Region
33/F, Revenue Tower
5 Gloucester Rd.
Wan Chai
Hong Kong

July 12, 2006

# TABLE OF CONTENTS

Page

# LIST OF FIGURES

Page

# LIST OF TABLES

# 1. INTRODUCTION

## 1.1 Study Objectives

The Desert Research Institute (DRI) assisted the Hong Kong Environmental Protection Department (HKEPD) with sampling support and analysis of $PM_{2.5}$ samples acquired over the course of one year from 11/03/04 to 10/29/05. The objectives of this study were to:

- Evaluate sampling and measurement methods for inorganic and organic particulate components and for gaseous precursors and end products of particle-forming atmospheric reactions.

- Determine the organic and inorganic composition of $PM_{2.5}$ and how it differs by season and proximity to different source types. Understand the atmospheric conditions causing $PM_{2.5}$ episodes.

- Based on ambient concentrations of marker compounds, source measurements performed elsewhere, and available Hong Kong emissions inventories, determine which sources are the most probable contributors to $PM_{2.5}$ in Hong Kong.

- Establish interannual variability of $PM_{2.5}$ concentration and chemical composition in Hong Kong urban and rural areas.

## 1.2 Background

The Hong Kong Environmental Protection Department (HKEPD) currently has not established, nor adopted ambient air-quality standards for fine particulate matter, particles with aerodynamic diameters less than 2.5 microns ($PM_{2.5}$). Current standards in Hong Kong reflect U.S. Environmental Protection Agency (EPA) National Ambient Air Quality Standards (NAAQS) for $PM_{10}$.

Chemically speciated $PM_{2.5}$ and $PM_{10}$ data from a 1998-99 pilot at Tsuen Wan, Hong Kong, showed that: 1) ~70% of $PM_{10}$ is in the $PM_{2.5}$ fraction, 2) carbonaceous aerosol and secondary ammonium sulfate constituted a major portion of $PM_{2.5}$, 3) $PM_{2.5}$ concentrations and compositions varied over twofold between the warm and cold seasons, and 4) elevated levels of organic carbon were the main contributor to elevated $PM_{2.5}$ concentrations during winter. These findings were confirmed by a 12-month $PM_{2.5}$ study carried out between 2000 and 2001. In addition, the 12-month study determined the contrast between urban and rural sites in Hong Kong, particularly with respect to carbonaceous material concentration (Louie et al., 2005a; 2005b).

Following the 12-month $PM_{2.5}$ study, another yearlong $PM_{2.5}$ monitoring project was completed. The object of this continuing study is to: 1) determining the interannual variability by comparing the first- and second-year $PM_{2.5}$ measurements, and 2) verify the hypothesis regarding the formation of $PM_{2.5}$ episodes. This report documents $PM_{2.5}$ measurements and data validation for this yearlong study. This data will be analyzed to characterize the composition and temporal and spatial variations of $PM_{2.5}$ concentrations.

## 1.3 Technical Approach

During the sampling period from 11/03/04 to 10/29/05, 24-hour $PM_{2.5}$ mass measurements were acquired every sixth day from the roadside-source-dominated Mong Kok (MK) site, the urban Tsuen Wan (TW) and Yuen Long (YL) sites, and the regional background Hok Tsui (HT) site. Two Partisol particle samplers (Rupprecht & Patashnick, Albany, NY) were used at each site to obtain $PM_{2.5}$ samples on both Teflon-membrane and quartz-fiber 47-mm filters. All sampled Teflon-membrane and quartz-fiber filters were analyzed for mass by gravimetry at HKEPD and then subjected to full chemical analysis at DRI as documented in Section 2.2.

## 1.4 Guide to Report

This section states the background and objectives of the Twelve Month Particulate Matter Study in Hong Kong. Section 2 documents the ambient monitoring network and the unified database compiled from these measurements. The ambient database is assembled, validated, and documented in Section 3. Section 4 compares the first- and second-year $PM_{2.5}$ measurement results. A report summary is provided in Section 5. The bibliography and references are assembled in Section 6.

# 2. SAMPLING NETWORK

## 2.1 Ambient Network

Twenty-four-hour $PM_{2.5}$ filter samples were taken at four sites in Hong Kong. Sampling took place every sixth day from 11/03/04 to 10/29/05. The ambient monitoring network shown in Figure 2-1 was designed to represent roadside (source), urban (receptor), and rural (background) areas that characterize $PM_{2.5}$ in Hong Kong. The sampling locations consisted of an urban roadside site at Mong Kok (MK), two urban sites at Tsuen Wan (TW) and Yuen Long (YL), and a rural regional background site at Hok Tsui (HT). Table 2-1 lists the site names, codes, locations, elevations, and a description of each site.

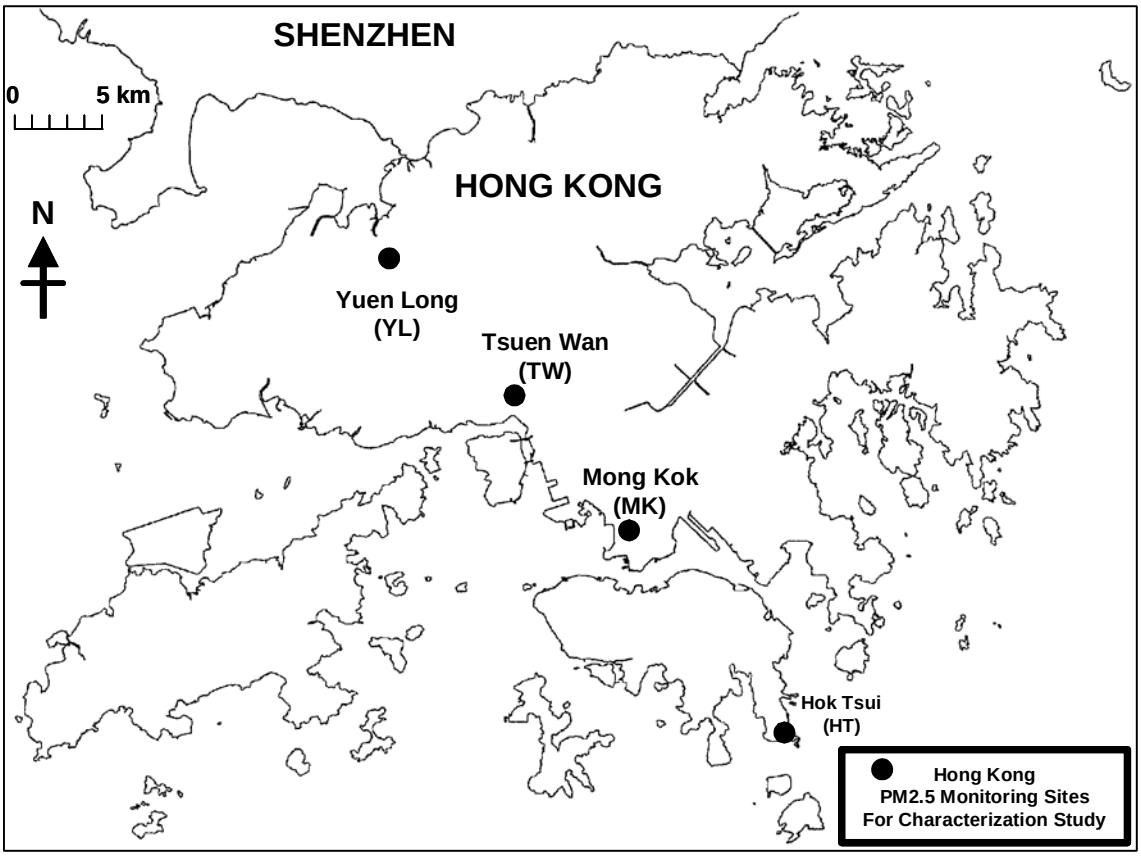


**Figure 2-1.** Map of the Hong Kong study area.

**Table 2-1.** Description of monitoring sites.

| Site Name (Code) and Location | Elevation above Mean Sea Level | Site Description |
|---|---|---|
| Mong Kok (MK)<br><br>Junction of Nathan Road and Lai Chi Kok Road. | ~8.5 m | An urban roadside site with mixed residential/commercial area surrounded by many tall buildings. |
| Tsuen Wan (TW)<br><br>Princess Alexandra Community Centre, 60 Tai Ho Road | ~21 m | An urban, densely populated, residential site with mixed commercial and industrial developments. Located northwest of the MK site. |
| Hok Tsui (HT)<br><br>Rural location | ~60 m | A rural background/transport site located about 20 km southeast of the MK site. |
| Yuen Long (YL)<br><br>269 Castle Peak Road | ~31 m | A northwestern town about 15 km southwest of Shenzhen. An industrial source is located ~1 km northeast of the monitoring site. |

## 2.2 Ambient Particulate Measurements

Two Rupprecht & Patashnick Partisol samplers were used at each site to acquire the ambient particulate air samples. The Partisol samplers were equipped with an Andersen SA-246 size-selective inlet/WINS impactor to sample $PM_{2.5}$ at a flow rate of 16.7 L/min. At this flow rate, a nominal volume of 24.1 $m^3$ of ambient air would be sampled over a 24-hour period. A vacuum pump drew ambient air through the inlet and down through the filter. The flow rate was controlled by a dry gas flow meter, downstream of the sample filter, and thus not affected by filter loading.

The Partisol samplers were configured to take either a Teflon-membrane filter or a quartz-fiber filter. Lippmann (1989), Lee and Ramamurthi (1993), Watson and Chow (1993; 1994), and Chow (1995) evaluated substrates for different sampling and analyses. Based on these evaluations, the filters chosen for this study were: 1) Pall Life Sciences (Ann Arbor,

MI) polymethylpentane ringed, 2.0-µm pore size, 47-mm diameter, PTFE Teflon-membrane filters (#R2PJ047) for mass and elemental analysis; and 2) Pall Life Sciences (Ann Arbor, MI) 47-mm diameter, pre-fired quartz-fiber filters (#2500QAT-UP) for carbon and ion analyses.

As shown in Figure 2-2, the Teflon-membrane filter collected particles for mass analysis by gravimetry and elemental analysis (40 elements including Na, Mg, Al, Si, P, S, Cl, K, Ca, Ti, V, Cr, Mn, Fe, Co, Ni, Cu, Zn, Ga, As, Se, Br, Rb, Sr, Y, Zr, Mo, Pd, Ag, Cd, In, Sn, Sb, Ba, La, Au, Hg, Tl, Pb, and U) by x-ray fluorescence (Watson et al., 1999). The quartz-fiber filter, also a 47-mm diameter filter, was analyzed for mass by gravimetry, for chloride ($Cl^-$), nitrate ($NO_3^-$), and sulfate ($SO_4^=$) by ion chromatography (Chow and Watson, 1999), for ammonium ($NH_4^+$) by automated colorimetry, for water-soluble sodium ($Na^+$) and potassium ($K^+$) by atomic absorption spectrophotometry, and for carbon by thermal evolution methods.

A major uncertainty in determining total carbon (TC) using thermal evolution methods results from differences in volatilization of certain organic compounds during sampling and storage (Fitz, 1990; Turpin et al., 1994; Chow et al., 1996). The split of organic and elemental carbon in thermal analysis, however, is even more ambiguous because it depends on temperature setpoints, temperature ramping rates, residence time at each setpoint, and combustion atmospheres. These parameters are only empirically defined. At higher combustion temperatures, samples visibly darken as OC pyrolyzes to EC in an oxygen-free environment. To overcome this problem, a laser is used to monitor changes in filter darkness during the thermal evolution process by detecting either filter reflectance (thermal/optical reflectance [TOR] method) or transmittance (thermal/optical transmittance [TOT] method).

The analytical protocol used in thermal evolution analysis of TC, OC, and EC in the National Park Service's IMPROVE network was used for this study. In the IMPROVE protocol, total carbon is divided into eight carbon fractions as a function of temperature and oxidation environment (Chow et al., 1993b; 2001; Watson et al., 1994). The temperature in a pure helium (He) atmosphere ramps from 25 to 120 °C (OC1), from 120 to 250 °C (OC2), from 250 to 450 °C (OC3), and from 450 to 550 °C (OC4). Then, a 98% He/2% $O_2$ atmosphere is introduced and peaks are integrated at 550 °C (EC1), 700 °C (EC2), and 800 °C (EC3). The fraction of pyrolyzed organic carbon (OPR or OPT) is detected in the He/$O_2$ atmosphere at 550 °C prior to the return of reflectance or transmittance to its original value. In the IMPROVE protocol, OC is defined as OC1+OC2+OC3+OC4+OPR, and EC is defined as the difference between TC and OC. The carbon analyses were performed with the DRI Model 2001 analyzer (Chen et al., 2004; Chow et al., 2004). Reflectance and transmittance charring correction are both reported in Table 3-1.

The Partisol samplers were operated and maintained by ENSR Environmental International Ltd. throughout the study duration. The flow rate was periodically audited to check for any flow discrepancies and to verify instrument performance. The Teflon-membrane and quartz-fiber filters were obtained prior to sampling by the HKEPD. The HKEPD was responsible for pre- and post-sampling procedures required for quality assurance and sample preservation. They were also responsible for conducting mass measurements and analysis on both filter types prior to shipping to DRI for chemical analysis.

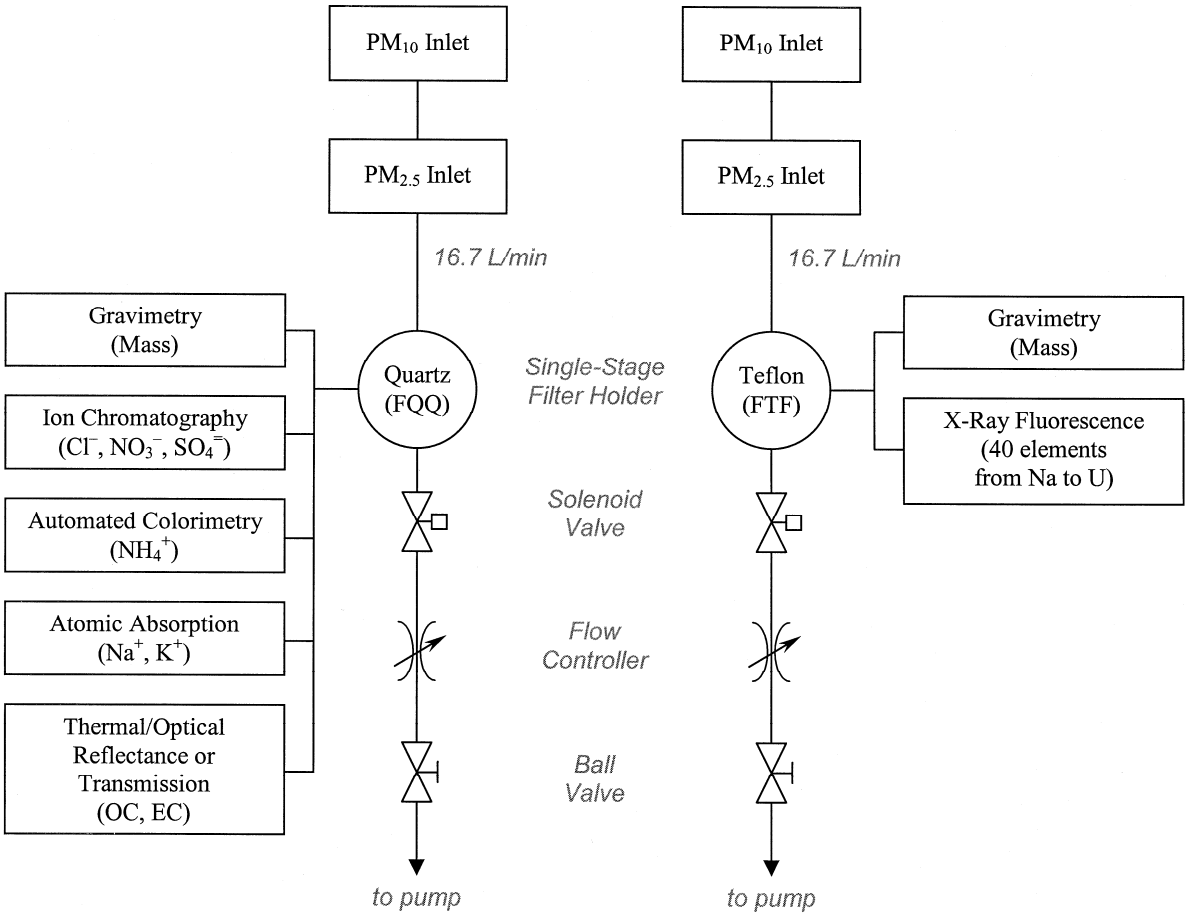


**Figure 2-2.** Schematic of $PM_{2.5}$ Partisol sampler configurations for the Twelve Month Particulate Matter Study in Hong Kong.

# 3. DATABASE AND DATA VALIDATION

This section evaluates the precision, accuracy, and validity of the Hong Kong $PM_{2.5}$ filter data measurements. Numerous air-quality studies have been conducted over the past decade, but the data obtained are often not available or applicable for data analysis and modeling, because the databases lack documentation with regard to sampling and analysis methods, quality-control/quality-assurance procedures, accuracy specifications, precision calculations, and data validity. Lioy et al. (1980), Chow and Watson (1989), Watson and Chow (1992), and Chow and Watson (1994) summarize the requirements, limitations, and current availability of ambient and source databases in the United States. The Hong Kong $PM_{2.5}$ data set intends to meet these requirements. The data files for these studies have the following attributes:

- They contain the ambient observables needed to assess source/receptor relationships.
- They are available in a well-documented, computerized form accessible by personal computers and over the Internet.
- Measurement methods, locations, and schedules are documented.
- Precision and accuracy estimates are reported.
- Validation flags are assigned.

This section introduces the features, data structures, and contents of the Hong Kong $PM_{2.5}$ data archive. The approach that was followed to obtain the final data files is illustrated in Figure 3-1. Detailed data-processing and data-validation procedures are documented in Section 3.4. These data are available in Microsoft Excel (.xls) format for convenient distribution to data users. The file extension identifies the file type according to the following definitions:

- TXT = ASCII text file
- DOC = Microsoft Word document
- XLS = Microsoft Excel spreadsheet

The assembled aerosol database for filter-pack measurements taken during the study is fully described by the file "HKEPDFLDNAME.XLS" (see Table 3-1) which documents variable names, descriptions, and measurement units.

**Database Structures and Features**

The raw HKEPD data was processed with Microsoft FoxPro 2.6 for Windows (Microsoft Corp., 1994), a commercially available relational database management system.

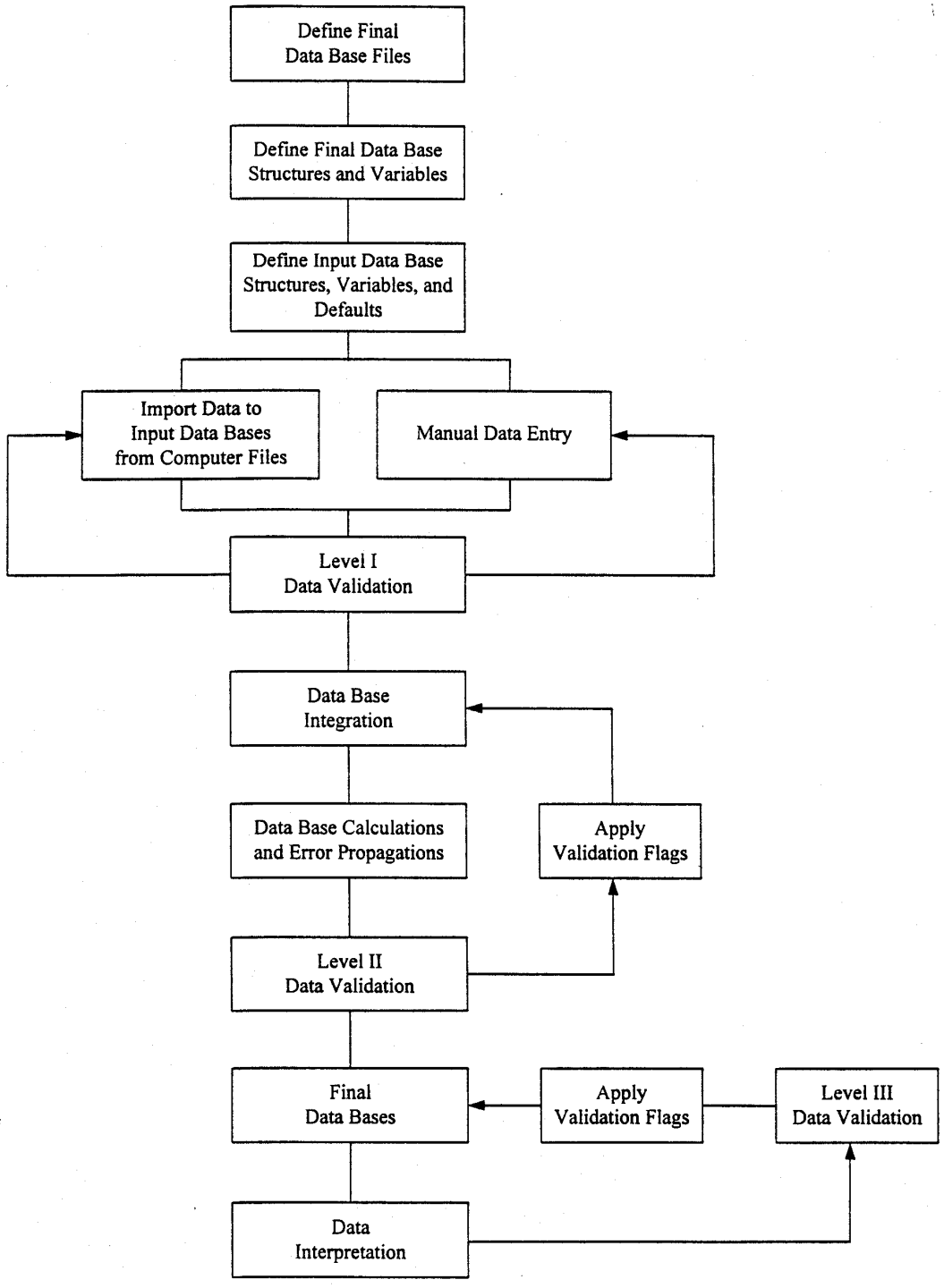


**Figure 3-1.** Flow diagram of the database management system.

**Table 3-1.** Variable names, descriptions, and measurement units in the assembled aerosol database for filter-pack measurements taken during the Twelve Month Particulate Matter Study in Hong Kong.

| Field Code | Description | Measurement Unit |
|---|---|---|
| SITE | Sampling site | |
| DATE | Sampling date | |
| SIZE | particle size cut | µm |
| TSAMPLEID | HKEPD sample ID | |
| TFILTERID | HKEPD Teflon filter ID | |
| TID | DRI Teflon filter ID | |
| QSAMPLEID | HKEPD sample ID | |
| QFILTERID | HKEPD quartz filter ID | |
| QID | DRI quartz filter ID | |
| TFFLG | Teflon filter field flag (see FLDFLAGS.doc) | |
| QFFLG | Quartz filter field flag (see FLDFLAGS.doc) | |
| ANIF | Anion analysis flag (see CHEMFLAG.doc) | |
| N4CF | Ammonium analysis flag (see CHEMFLAG.doc) | |
| NAAF | Soluble sodium analysis flag (see CHEMFLAG.doc) | |
| KPAF | Soluble potassium analysis flag (see CHEMFLAG.doc) | |
| OETF | IMPROVE Carbon analysis flag (see CHEMFLAG.doc) | |
| ELXF | XRF analysis flag (see CHEMFLAG.doc) | |
| TVOC | Teflon filter volume | $m^3$ |
| TVOU | Teflon filter volume uncertainty (estimated at 5% of volume) | $m^3$ |
| QVOC | Quartz filter volume | $m^3$ |
| QVOU | Quartz filter volume uncertainty (estimated at 5% of volume) | $m^3$ |
| MSGC | Teflon Mass concentration | $\mu g/m^3$ |
| MSGU | Teflon Mass concentration uncertainty | $\mu g/m^3$ |
| QMSGC | QMA Mass concentration | $\mu g/m^3$ |
| QMSGU | QMA Mass concentration uncertainty | $\mu g/m^3$ |
| CLIC | Chloride concentration | $\mu g/m^3$ |
| CLIU | Chloride concentration uncertainty | $\mu g/m^3$ |
| N3IC | Nitrate concentration | $\mu g/m^3$ |
| N3IU | Nitrate concentration uncertainty | $\mu g/m^3$ |
| S4IC | Sulfate concentration | $\mu g/m^3$ |
| S4IU | Sulfate concentration uncertainty | $\mu g/m^3$ |
| N4CC | Ammonium concentration | $\mu g/m^3$ |
| N4CU | Ammonium concentration uncertainty | $\mu g/m^3$ |
| NAAC | Soluble Sodium concentration | $\mu g/m^3$ |
| NAAU | Soluble Sodium concentration uncertainty | $\mu g/m^3$ |
| KPAC | Soluble Potassium concentration | $\mu g/m^3$ |
| KPAU | Soluble Potassium concentration uncertainty | $\mu g/m^3$ |
| O1TC | Organic Carbon Fraction 1concentration | $\mu g/m^3$ |
| O1TU | Organic Carbon Fraction 1 concentration uncertainty | $\mu g/m^3$ |
| O2TC | Organic Carbon Fraction 2 concentration | $\mu g/m^3$ |
| O2TU | Organic Carbon Fraction 2 concentration uncertainty | $\mu g/m^3$ |
| O3TC | Organic Carbon Fraction 3 concentration | $\mu g/m^3$ |
| O3TU | Organic Carbon Fraction 3 concentration uncertainty | $\mu g/m^3$ |
| O4TC | Organic Carbon Fraction 4 concentration | $\mu g/m^3$ |
| O4TU | Organic Carbon Fraction 4 concentration uncertainty | $\mu g/m^3$ |

**Table 3-1.** (continued)

| Field Code | Description | Measurement Unit |
|---|---|---|
| OPTTC | Pyrolyzed Organic Carbon concentration (Laser transmittance) | $\mu g/m^3$ |
| OPTTU | Pyrolyzed Organic Carbon concentration uncertainty | $\mu g/m^3$ |
| OPTRC | Pyrolyzed Organic Carbon concentration (Laser reflectance) | $\mu g/m^3$ |
| OPTRU | Pyrolyzed Organic Carbon concentration uncertainty | $\mu g/m^3$ |
| OCTTC | Organic Carbon concentration (Laser transmittance) | $\mu g/m^3$ |
| OCTTU | Organic Carbon concentration uncertainty | $\mu g/m^3$ |
| OCTRC | Organic Carbon concentration (Laser reflectance) | $\mu g/m^3$ |
| OCTRU | Organic Carbon concentration uncertainty | $\mu g/m^3$ |
| E1TC | Elemental Carbon Fraction 1 concentration | $\mu g/m^3$ |
| E1TU | Elemental Carbon Fraction 1 concentration uncertainty | $\mu g/m^3$ |
| E2TC | Elemental Carbon Fraction 2 concentration | $\mu g/m^3$ |
| E2TU | Elemental Carbon Fraction 2 concentration uncertainty | $\mu g/m^3$ |
| E3TC | Elemental Carbon Fraction 3 concentration | $\mu g/m^3$ |
| E3TU | Elemental Carbon Fraction 3 concentration uncertainty | $\mu g/m^3$ |
| ECTTC | Elemental Carbon concentration (Laser transmittance) | $\mu g/m^3$ |
| ECTTU | Elemental Carbon concentration uncertainty | $\mu g/m^3$ |
| ECTRC | Elemental Carbon concentration (Laser reflectance) | $\mu g/m^3$ |
| ECTRU | Elemental Carbon concentration uncertainty | $\mu g/m^3$ |
| TCTC | Total Carbon concentration | $\mu g/m^3$ |
| TCTU | Total Carbon concentration uncertainty | $\mu g/m^3$ |
| NAXC | Sodium concentration | $\mu g/m^3$ |
| NAXU | Sodium concentration uncertainty | $\mu g/m^3$ |
| MGXC | Magnesium concentration | $\mu g/m^3$ |
| MGXU | Magnesium concentration uncertainty | $\mu g/m^3$ |
| ALXC | Aluminum concentration | $\mu g/m^3$ |
| ALXU | Aluminum concentration uncertainty | $\mu g/m^3$ |
| SIXC | Silicon concentration | $\mu g/m^3$ |
| SIXU | Silicon concentration uncertainty | $\mu g/m^3$ |
| PHXC | Phosphorous concentration | $\mu g/m^3$ |
| PHXU | Phosphorous concentration uncertainty | $\mu g/m^3$ |
| SUXC | Sulfur concentration | $\mu g/m^3$ |
| SUXU | Sulfur concentration uncertainty | $\mu g/m^3$ |
| CLXC | Chlorine concentration | $\mu g/m^3$ |
| CLXU | Chlorine concentration uncertainty | $\mu g/m^3$ |
| KPXC | Potassium concentration | $\mu g/m^3$ |
| KPXU | Potassium concentration uncertainty | $\mu g/m^3$ |
| CAXC | Calcium concentration | $\mu g/m^3$ |
| CAXU | Calcium concentration uncertainty | $\mu g/m^3$ |
| TIXC | Titanium concentration | $\mu g/m^3$ |
| TIXU | Titanium concentration uncertainty | $\mu g/m^3$ |
| VAXC | Vanadium concentration | $\mu g/m^3$ |
| VAXU | Vanadium concentration uncertainty | $\mu g/m^3$ |
| CRXC | Chromium concentration | $\mu g/m^3$ |
| CRXU | Chromium concentration uncertainty | $\mu g/m^3$ |
| MNXC | Manganese concentration | $\mu g/m^3$ |
| MNXU | Manganese concentration uncertainty | $\mu g/m^3$ |
| FEXC | Iron concentration | $\mu g/m^3$ |
| FEXU | Iron concentration uncertainty | $\mu g/m^3$ |

**Table 3-1.** (continued)

| Field Code | Description | Measurement Unit |
|---|---|---|
| COXC | Cobalt concentration | $\mu g/m^3$ |
| COXU | Cobalt concentration uncertainty | $\mu g/m^3$ |
| NIXC | Nickel concentration | $\mu g/m^3$ |
| NIXU | Nickel concentration uncertainty | $\mu g/m^3$ |
| CUXC | Copper concentration | $\mu g/m^3$ |
| CUXU | Copper concentration uncertainty | $\mu g/m^3$ |
| ZNXC | Zinc concentration | $\mu g/m^3$ |
| ZNXU | Zinc concentration uncertainty | $\mu g/m^3$ |
| GAXC | Gallium concentration | $\mu g/m^3$ |
| GAXU | Gallium concentration uncertainty | $\mu g/m^3$ |
| ASXC | Arsenic concentration | $\mu g/m^3$ |
| ASXU | Arsenic concentration uncertainty | $\mu g/m^3$ |
| SEXC | Selenium concentration | $\mu g/m^3$ |
| SEXU | Selenium concentration uncertainty | $\mu g/m^3$ |
| BRXC | Bromine concentration | $\mu g/m^3$ |
| BRXU | Bromine concentration uncertainty | $\mu g/m^3$ |
| RBXC | Rubidium concentration | $\mu g/m^3$ |
| RBXU | Rubidium concentration uncertainty | $\mu g/m^3$ |
| SRXC | Strontium concentration | $\mu g/m^3$ |
| SRXU | Strontium concentration uncertainty | $\mu g/m^3$ |
| YTXC | Yttrium concentration | $\mu g/m^3$ |
| YTXU | Yttrium concentration uncertainty | $\mu g/m^3$ |
| ZRXC | Zirconium concentration | $\mu g/m^3$ |
| ZRXU | Zirconium concentration uncertainty | $\mu g/m^3$ |
| MOXC | Molybdenum concentration | $\mu g/m^3$ |
| MOXU | Molybdenum concentration uncertainty | $\mu g/m^3$ |
| PDXC | Palladium concentration | $\mu g/m^3$ |
| PDXU | Palladium concentration uncertainty | $\mu g/m^3$ |
| AGXC | Silver concentration | $\mu g/m^3$ |
| AGXU | Silver concentration uncertainty | $\mu g/m^3$ |
| CDXC | Cadmium concentration | $\mu g/m^3$ |
| CDXU | Cadmium concentration uncertainty | $\mu g/m^3$ |
| INXC | Indium concentration | $\mu g/m^3$ |
| INXU | Indium concentration uncertainty | $\mu g/m^3$ |
| SNXC | Tin concentration | $\mu g/m^3$ |
| SNXU | Tin concentration uncertainty | $\mu g/m^3$ |
| SBXC | Antimony concentration | $\mu g/m^3$ |
| SBXU | Antimony concentration uncertainty | $\mu g/m^3$ |
| BAXC | Barium concentration | $\mu g/m^3$ |
| BAXU | Barium concentration uncertainty | $\mu g/m^3$ |
| LAXC | Lanthanum concentration | $\mu g/m^3$ |
| LAXU | Lanthanum concentration uncertainty | $\mu g/m^3$ |
| AUXC | Gold concentration | $\mu g/m^3$ |
| AUXU | Gold concentration uncertainty | $\mu g/m^3$ |
| HGXC | Mercury concentration | $\mu g/m^3$ |
| HGXU | Mercury concentration uncertainty | $\mu g/m^3$ |
| TLXC | Thallium concentration | $\mu g/m^3$ |
| TLXU | Thallium concentration uncertainty | $\mu g/m^3$ |

**Table 3-1.** (continued)

| Field Code | Description | Measurement Unit |
|---|---|---|
| PBXC | Lead concentration | $\mu g/m^3$ |
| PBXU | Lead concentration uncertainty | $\mu g/m^3$ |
| URXC | Uranium concentration | $\mu g/m^3$ |
| URXU | Uranium concentration uncertainty | $\mu g/m^3$ |

FoxPro can handle 256 fields of up to 4,000 characters per record and up to one billion records per file. This system can be implemented on most IBM PC-compatible desktop computers. The database files (*.DBF) can also be read directly into a variety of popular statistical, plotting, database, and spreadsheet programs without having to use any specific conversion software. After processing, the final HKEPD data was converted from FoxPro to Microsoft Excel format for reporting ease and general use purposes.

In FoxPro, one of five field types (character, date, numerical, logical, or memo) was assigned to each observable. Sampling sites and particle size fractions are defined as "Character" fields, sampling dates are defined as "Date" fields, and measured data are defined as "Numeric" fields. "Logical" fields are used to represent a "yes" or "no" value applied to a variable, and "Memo" fields accommodate large blocks of textual information and are used to document the data validation results.

Data contained in different XBase files can be linked by indexing on and relating to common attributes in each file. Sampling site, sampling hour, sampling period, particle size, and sampling substrate IDs are, typically, the common fields among various data files that can be used to relate data in one file to the corresponding data in another file. To assemble the final data files, information was merged from many data files derived from field monitoring and laboratory analyses by relating information on the common fields cited above.

Table 3-2 lists the contents of the final data file. Each observable is identified by a field name which follows a pattern for that type of observable. For example, in the filter-based aerosol concentration file, the first two characters represent the measured species (e.g., AL for aluminum, SI for silicon, CA for calcium), the third character designates the analysis method (i.e., "G" for gravimetric weighing, "X" for x-ray fluorescence analysis, "I" for ion chromatography, "A" for atomic absorption spectrophotometry, "C" for automated colorimetry, "T" for thermal/optical carbon analysis), and the last character uses a "C" to identify a species concentration or a "U" to identify the uncertainty (i.e., precision) of the corresponding measurement. Each measurement method is associated with a separate validation field to document the sample validity for that method. Missing or invalidated measurements have been removed and replaced with –99. All times show the start and end of the sampling period.

**Table 3-2.** Summary of $PM_{2.5}$ data files for the Twelve Month Particulate Matter Study in Hong Kong.

| Category | Database File | Database Description |
|---|---|---|
| I. DATABASE DOCUMENTATION | | |
| | HKEPDFLDNAME.XLS | Defines the field names, measurement units, and formats used in the ambient database |
| II. MASS AND CHEMICAL DATA | | |
| | HKEPD- PM25.XLS | Contains 24-hour $PM_{2.5}$ mass and chemical data[a,b] collected with partisol filter samplers at four sites on every sixth day between 11/03/04 and 10/29/05. |
| III. DATABASE VALIDATION | | |
| | FLDFLAGS.DOC | Contains the field sampling data validation flags |
| | CHEMFLAG.DOC | Contains the chemical analysis data validation flags |

[a] Includes 40 elements (Na, Mg, Al, Si, P, S, Cl, K, Ca, Ti, V, Cr, Mn, Fe, Co, Ni, Cu, Zn, Ga, As, Se, Br, Rb, Sr, Y, Zr, Mo, Pd, Ag, Cd, In, Sn, Sb, Ba, La, Au, Hg, Tl, Pb, and U) by x-ray fluorescence.

[b] Includes chloride, nitrate, and sulfate by ion chromatography; ammonium by automated colorimetry; water-soluble sodium and potassium by atomic absorption spectrophotometry; and organic carbon, elemental carbon, eight carbon fractions (OC1, OC2, OC3, OC4, OP, EC1, EC2, and EC3) by thermal/optical reflectance following the IMPROVE protocol.

## 3.1 Measurement and Analytical Specifications

Every measurement consists of: 1) a value; 2) a precision; 3) an accuracy; and 4) a validity (Hidy, 1985; Watson et al., 1989; 2001). The measurement methods described in Section 2 are used to obtain the value. Performance testing via regular submission of standards, blank analysis, and replicate analysis are used to estimate precision. These precisions are reported in the data files described in Section 3.1 so that they can be propagated through air-quality models and used to evaluate how well different values compare with one another. The submission and evaluation of independent standards through quality audits are used to estimate accuracy. Validity applies both to the measurement method and to each measurement taken with that method. The validity of each measurement is indicated by appropriate flagging within the data base, while the validity of the methods has been evaluated in this study by tests described in Section 3.4.

### 3.1.1 Definitions of Measurement Attributes

The precision, accuracy, and validity of the Twelve Month Particulate Matter Study in Hong Kong aerosol measurements are defined as follows (Chow et al., 1993a):

- A **measurement** is an observation at a specific time and place which possesses: 1) value – the center of the measurement interval; 2) precision – the width of the

measurement interval; 3) accuracy – the difference between measured and reference values; and 4) validity – the compliance with assumptions made in the measurement method.

A **measurement method** is the combination of equipment, reagents, and procedures, which provide the value of a measurement. The full description of the measurement method requires substantial documentation. For example, two methods may use the same sampling systems and the same analysis systems. These are not identical methods, however, if one performs acceptance testing on filter media and the other does not. Seemingly minor differences between methods can result in major differences between measurement values.

- **Measurement method validity** is the identification of measurement method assumptions, the quantification of effects of deviations from those assumptions, the evaluation that deviations are within reasonable tolerances for the specific application, and the creation of procedures to quantify and minimize those deviations during a specific application.

- **Sample validation** is accomplished by procedures that identify deviations from measurement assumptions and the assignment of flags to individual measurements for potential deviations from assumptions.

- The **comparability and equivalence of sampling and analysis methods** are established by the comparison of values and precisions for the same measurement obtained by different measurement methods. Interlaboratory and intralaboratory comparisons are usually made to establish this comparability. Simultaneous measurements of the same observable are considered equivalent when more than 90% of the values differ by no more than the sum of two one-sigma precision intervals for each measurement.

- **Completeness** measures how many environmental measurements with specified values, precisions, accuracies, and validities were obtained out of the total number attainable. It measures the practicability of applying the selected measurement processes throughout the measurement period. Databases which have excellent precision, accuracy, and validity may be of little use if they contain so many missing values that data interpretation is impossible.

A total of 244 ambient filter samples were acquired during this study, and submitted for comprehensive chemical analyses. This resulted in about 25,000 data points, as documented in Section 3.1. All of the 244 ambient aerosol samples acquired during the study were considered valid after data validation and final review. In addition, complete chemical analysis was completed on 95 field blanks, 60 lab blanks and 48 precision check samples.

A database with numerous data points, such as the one generated from this study, requires detailed documentation of precision, accuracy, and validity of the measurements. The next section addresses the procedures followed to define these quantities and presents the results of the procedures.

### 3.1.2 Definitions of Measurement Precision

Measurement precisions were propagated from precisions of the volumetric measurements, the chemical composition measurements, and the field blank variability using the methods of Bevington (1969) and Watson et al. (2001). Let $i = 1,\mathrm{K}\,, p$ represent the number of species, and $j = 1,\mathrm{K}\,, n$ represent the number of samples. Then the following equations calculated the precision associated with filter-based measurements of $p$ species over $n$ samples:

$$V = F \cdot t \tag{3-1}$$

$$C_i = \frac{M_i - B_i}{V} \tag{3-2}$$

$$B_i = \begin{cases} \dfrac{1}{n}\displaystyle\sum_{j=1}^{n} B_{ij}, & B_i > \sigma_{B_i} \\ 0, & B_i \le \sigma_{B_i} \end{cases} \tag{3-3}$$

$$\sigma_{B_i} = \max\left\{ \sqrt{\frac{1}{n-1}\sum_{j=1}^{n}\left(B_{ij} - B_i\right)^2}\,, \sqrt{\frac{1}{n}\sum_{j=1}^{n} B_{ij}^2} \right\} \tag{3-4}$$

$$\sigma_{C_i} = \sqrt{\frac{\sigma_{M_i}^2 + \sigma_{B_i}^2}{V^2} + \frac{\sigma_V^2\left(M_i - B_i\right)^2}{V^4}} \tag{3-5}$$

$$\sigma_{RMS_i} = \sqrt{\frac{1}{n}\sum_{j=1}^{n}\sigma_{C_i}^2} \tag{3-6}$$

$$\sigma_V / V = 0.05 \tag{3-7}$$

where:

$V =$ volume of air sampled

$F =$ flow rate throughout sampling period

$t =$ sample duration

$C_i =$ the ambient concentration of species $i$

$M_i =$ amount of species $i$ on the substrate

$B_i =$ average amount of species $i$ on field blanks

$B_{ij} =$ the amount of species $i$ found on field blank $j$

$\sigma_{B_i} =$ blank precision for species $i$

$\sigma_{C_i} =$ propagated precision for the concentration of species $i$

$\sigma_{M_i} =$ precision of amount of species $i$ on the substrate

$\sigma_V =$ precision of sample volume

$\sigma_{RMS_i}$ = root mean square precision for species $i$

Dynamic field blanks were periodically placed in each sampling system without air being drawn through them to estimate the magnitude of passive deposition for the period of time which filter packs remained in a sampler (typically 24 hours). No statistically significant inter-site differences in field blank concentrations were found for any species after removal of outliers (i.e., concentration exceeding three times the standard deviations of the field blanks). The average field blank concentrations (with outliers removed) were calculated for each species on each substrate (e.g., Teflon-membrane, quartz-fiber), irrespective of the sites.

**Analytical Specifications**

Blank precisions ($\sigma_{Bi}$) are defined as the higher value of the standard deviation of the blank measurements, $STD_{Bi}$, or the square root of the averaged squared uncertainties of the blank concentrations, $SIG_{Bi}$. If the average blank for a species was less than its precision, the blank was set to zero (as shown in Equation 3-3). Dynamic field-blank concentrations in µg/filter are given in Table 3-3 for $PM_{2.5}$ samples collected during the study.

The precisions ($\sigma_{Mi}$) for x-ray fluorescence analysis were determined from counting statistics unique to each sample. Hence, the $\sigma_{Mi}$ is a function of the energy-specific peak area, the background, and the area under the baseline.

As shown in Table 3-3, the standard deviation of the field blank is more than twice its corresponding root mean square error (RMSE) for soluble sodium ($Na^+$) and soluble potassium ($K^+$). Some of these field blanks may have been contaminated during the passive deposition period and during sample changing while exposed to ambient conditions. By examining the individual field blank values, it is shown that these values are well within the range of the standard deviation of the average blank concentrations and therefore are assumed valid and representative.

$PM_{2.5}$ Teflon mass blank values averaged 0.24±4.5 µg/47-mm filter. The quartz mass blank values averaged -2.4±7.3 µg/47-mm filter. Filter mass and blank mass analysis were performed by the HKEPD. Mass blank subtractions and calculated uncertainties were not examined by DRI and were thus not included in Tables 3-3 and 3-4. The largest variation was found for soluble sodium, with an average of 21.9±2.8 µg/47-mm filter. This large standard deviation in blank samples was mainly due to the adsorption of sodium species during the passive sampling period when filters were left in the sampler before and after sampling. The proximity of the sampling sites to the ocean (<1 km) supports this assumption. These deviations were equivalent for both field and laboratory filter blanks.

Table 3-4 summarizes the analytical specifications for the 24-hour $PM_{2.5}$ measurements obtained during the study. Minimum detectable limits (MDL), root mean squared (RMS) precisions, and lower quantifiable limits (LQL) are given. The MDL is defined as the concentration at which the instrument response equals three times the standard deviation of the response to a known concentration of zero. RMS precision is the square root of the averaged squared uncertainties. The LQL is defined as a concentration corresponding to three times the standard deviation of the dynamic field blank. The LQLs in Table 3-4 were divided by 24.1 $m^3$, nominal 24-hour volume, for the Partisol samplers. Actual volumes varied from sample to sample, but were typically within ±5% of the pre-set volume.

The LQLs should always be equal to or larger than the analytical MDLs, because they include the standard deviation of the field blank and flow rate precision (Watson et al., 2001). This was the case for most of the chemical compounds noted in Table 3-4. This table also indicates that the RMS precisions were comparable in magnitude to the LQLs for most species.

The number of reported (nonvoid, nonmissing) concentrations for each species and the number of reported concentrations greater than the MDLs and LQLs are also summarized in Table 3-4. For the study samples, mass, ions (e.g., nonvolatilized nitrate, sulfate, ammonium, and soluble potassium), organic and elemental carbon, sulfur, and lead were detected in almost all samples (greater than 95%). Chloride and soluble sodium were detected in 64% and 100% of the samples, respectively. Several transition metals (e.g., Co, Y, Zr, Mo, Pd, Ag, Cd, Au, and Hg) were not detected in most of the samples (less than 5%). This is typical for urban and non-urban sites in most regions. Other transition metals, such as titanium (Ti), chromium (Cr), copper (Cu), gallium (Ga), arsenic (As), selenium (Se), rubidium (Rb), strontium (Sr), tin (Sn) and, barium (Ba), were detected in 91%, 50%, 89%, 7%, 57%, 18%, 42%, 8% 41%, and 7% of the analyzed samples, respectively. Residual-oil-related species, such as nickel (Ni) and vanadium (V), were detected in 91% and 100% of the samples, respectively. Industrial-source-related toxic species, such as mercury (Hg) and cadmium (Cd), were only detected in 2% and 4% of the samples, respectively. The maximum arsenic (As) concentration of 0.0407 $\mu g/m^3$ is a fairly high value, being over 20 times higher than the maximum concentration measured during the 2000-01 Southern Nevada Air Quality Study (SNAQS; Green et al., 2002) in the U.S. Crustal-related species such as aluminum (Al), silicon (Si), potassium (K), calcium (Ca), iron (Fe), and zinc (Zn) were found above the LQLs in over 93% of the samples. Motor-vehicle-related species, such as bromine (Br) and lead (Pb), were detected in 80% and 83% of the samples, respectively. Chlorine was detected in over 86% of the samples.

**Table 3-3.** $PM_{2.5}$ Partisol dynamic field blank concentrations at the MK, TW and HT sites during the Twelve Month Particulate Matter Study in Hong Kong.

| | Concentrations in µg/47-mm filter | | | | | |
|---|---|---|---|---|---|---|
| Species | Blank Subtracted[a] ($B_i$) | Blank Subtracted Precision[b] ($S_{Bi}$) | Average Field Blank | Field Blank Std. Dev. ($STD_{Bi}$) | RMS Blank Precision[c] ($S_{RMS}$) | Total No. of Blanks in Average |
| Teflon Mass | 0.0000 | 4.4705 | 0.2361 | 4.4705 | N/A | 72 |
| Quartz Mass | 0.0000 | 7.2550 | -2.3889 | 7.2550 | N/A | 72 |
| Chloride ($Cl^-$) | 0.3721 | 1.0422 | 0.5977 | 0.8583 | 0.5052 | 96 |
| Nitrate ($NO_3^-$) | 0.0000 | 0.5924 | 0.3499 | 0.4806 | 0.5002 | 96 |
| Sulfate ($SO_4^=$) | 3.1767 | 3.7254 | 3.1767 | 1.9563 | 0.5129 | 96 |
| Ammonium ($NH4^+$) | 0.3086 | 0.5305 | 0.5040 | 0.1663 | 0.5000 | 96 |
| Soluble Sodium ($Na^+$) | 21.9375 | 22.1168 | 21.9375 | 2.8253 | 0.1469 | 96 |
| Soluble Potassium ($K^+$) | 0.3908 | 0.4017 | 0.3908 | 0.0935 | 0.0502 | 96 |
| **IMPROVE PROTOCOL** | | | | | | |
| O1TC | 1.6162 | 1.9911 | 1.6862 | 1.2447 | 0.6002 | 87 |
| O2TC | 5.2261 | 5.1107 | 5.1699 | 1.4556 | 0.9774 | 87 |
| O3TC | 6.5320 | 6.4353 | 6.5114 | 1.8268 | 2.5257 | 87 |
| O4TC | 0.0000 | 0.7534 | 0.4803 | 0.6327 | 0.8905 | 87 |
| OPTTC | 0.0000 | 0.6472 | 0.2390 | 0.6401 | 0.6607 | 87 |
| OPTRC | 0.0000 | 0.0000 | 0.0000 | 0.0000 | 0.6400 | 87 |
| OCTTC | 14.2395 | 14.0876 | 14.0875 | 4.5579 | 3.6591 | 87 |
| OCTRC | 14.0193 | 13.7741 | 13.8483 | 4.2166 | 3.6601 | 87 |
| E1TC | 0.0000 | 0.3812 | 0.0852 | 0.3812 | 0.4812 | 87 |
| E2TC | 0.0000 | 0.6174 | 0.3721 | 0.5343 | 0.6073 | 87 |
| E3TC | 0.0000 | 0.3076 | 0.0462 | 0.3076 | 0.2851 | 87 |
| ECTTC | 0.0000 | 0.7612 | 0.2644 | 0.7590 | 0.7621 | 87 |
| ECTRC | 0.0000 | 1.0047 | 0.5033 | 0.9330 | 0.7681 | 87 |
| TCTC | 14.4856 | 14.3563 | 14.3515 | 4.6592 | 3.8415 | 87 |
| Sodium (Na) | 0.0000 | 0.7254 | 0.1240 | 0.7185 | 0.7532 | 96 |
| Magnesium (Mg) | 0.0000 | 0.3455 | 0.0617 | 0.3417 | 0.8351 | 96 |
| Aluminum (Al) | 0.0000 | 0.1683 | 0.0454 | 0.1629 | 0.5641 | 96 |
| Silicon (Si) | 0.0000 | 0.2439 | 0.0736 | 0.2338 | 0.2590 | 96 |
| Phosphorus (P) | 0.0000 | 0.0357 | -0.0128 | 0.0335 | 0.0520 | 96 |
| Sulfur (S) | 0.0000 | 0.0439 | -0.0034 | 0.0439 | 0.0137 | 96 |
| Chlorine (Cl) | 0.0000 | 0.0382 | 0.0079 | 0.0376 | 0.0386 | 96 |
| Potassium (K) | 0.0000 | 0.0678 | -0.0010 | 0.0678 | 0.0030 | 96 |
| Calcium (Ca) | 0.0000 | 0.0326 | 0.0147 | 0.0293 | 0.0453 | 96 |
| Titanium (Ti) | 0.0000 | 0.0161 | 0.0060 | 0.0150 | 0.0268 | 96 |

**Table 3-3.** (continued)

| Species | Concentrations in µg/47-mm filter | | | | | |
|---|---|---|---|---|---|---|
| | Blank Subtracted[a] ($B_i$) | Blank Subtracted Precision[b] ($S_{Bi}$) | Average Field Blank | Field Blank Std. Dev. ($STD_{Bi}$) | RMS Blank Precision[c] ($S_{RMS}$) | Total No. of Blanks in Average |
| Vanadium (V) | 0.0000 | 0.0058 | 0.0009 | 0.0058 | 0.0101 | 96 |
| Chromium (Cr) | 0.0000 | 0.0102 | -0.0009 | 0.0102 | 0.0419 | 96 |
| Manganese (Mn) | 0.0000 | 0.0323 | 0.0006 | 0.0323 | 0.1192 | 96 |
| Iron (Fe) | 0.0000 | 0.2384 | 0.0331 | 0.2374 | 0.1780 | 96 |
| Cobalt (Co) | 0.0000 | 0.0119 | 0.0004 | 0.0119 | 0.0201 | 96 |
| Nickel (Ni) | 0.0000 | 0.0110 | 0.0010 | 0.0110 | 0.0319 | 96 |
| Copper (Cu) | 0.0000 | 0.0159 | 0.0034 | 0.0156 | 0.0252 | 96 |
| Zinc (Zn) | 0.0000 | 0.0446 | 0.0059 | 0.0444 | 0.0337 | 96 |
| Gallium (Ga) | 0.0000 | 0.0691 | 0.0057 | 0.0691 | 0.1023 | 96 |
| Arsenic (As) | 0.0000 | 0.0087 | 0.0004 | 0.0087 | 0.0268 | 96 |
| Selenium (Se) | 0.0000 | 0.0000 | 0.0000 | 0.0000 | 0.0235 | 96 |
| Bromine (Br) | 0.0000 | 0.0274 | 0.0036 | 0.0273 | 0.0268 | 96 |
| Rubidium (Rb) | 0.0000 | 0.0151 | 0.0000 | 0.0151 | 0.0252 | 96 |
| Strontium (Sr) | 0.0000 | 0.0279 | -0.0052 | 0.0275 | 0.0590 | 96 |
| Yttrium (Y) | 0.0000 | 0.0190 | 0.0007 | 0.0190 | 0.0385 | 96 |
| Zirconium (Zr) | 0.0000 | 0.0531 | 0.0046 | 0.0531 | 0.0805 | 96 |
| Molybdenum (Mo) | 0.0000 | 0.0412 | 0.0026 | 0.0412 | 0.0858 | 96 |
| Palladium (Pd) | 0.0000 | 0.0639 | 0.0235 | 0.0598 | 0.1158 | 96 |
| Silver (Ag) | 0.0000 | 0.0582 | 0.0119 | 0.0573 | 0.0888 | 96 |
| Cadmium (Cd) | 0.0000 | 0.0747 | 0.0001 | 0.0747 | 0.0989 | 96 |
| Indium (In) | 0.0000 | 0.0739 | -0.0118 | 0.0733 | 0.0957 | 96 |
| Tin (Sn) | 0.0000 | 0.0943 | -0.0045 | 0.0943 | 0.1141 | 96 |
| Antimony (Sb) | 0.0000 | 0.1287 | 0.0178 | 0.1281 | 0.1029 | 96 |
| Barium (Ba) | 0.0000 | 0.1654 | -0.0089 | 0.1654 | 0.2483 | 96 |
| Lanthanum (La) | 0.0000 | 0.3994 | 0.1445 | 0.3743 | 0.5143 | 96 |
| Gold (Au) | 0.0000 | 0.0688 | 0.0010 | 0.0688 | 0.1157 | 96 |
| Mercury (Hg) | 0.0000 | 0.0180 | 0.0021 | 0.0180 | 0.0436 | 96 |
| Thallium (Tl) | 0.0000 | 0.0403 | -0.0085 | 0.0397 | 0.0889 | 96 |
| Lead (Pb) | 0.0000 | 0.0360 | 0.0097 | 0.0348 | 0.0855 | 96 |
| Uranium (U) | 0.0000 | 0.0735 | 0.0087 | 0.0734 | 0.1139 | 96 |

** DRI did not conduct filter mass analysis. Estimated mass precision is given.

[a] Values used in data processing. Non-zero average blank concentrations are subtracted when the average blank exceeds its standard deviation.

[b] Larger of either the analytical precision or standard deviation from the field.

[c] RMS precision is the square root of the sum of the squared uncertainties of the observations divided by the number of observations.

**Table 3-4.** Analytical specifications for 24-hour $PM_{2.5}$ measurements at the MK, TW, and HT sites during the Twelve Month Particulate Matter Study in Hong Kong.

| Species | Analysis Method[a] | MDL[b] (µg/m$^3$) | RMS[c] (µg/m$^3$) | LQL[d] (µg/m$^3$) | No.of Values | No. > MDL | % > MDL | No. > LQL | % > LQL |
|---|---|---|---|---|---|---|---|---|---|
| Teflon Mass | Gravimetry | N/A | N/A | 0.5588 | 244 | N/A | N/A | 244 | 100.0 |
| Quartz Mass | Gravimetry | N/A | N/A | 0.9069 | 244 | N/A | N/A | 244 | 100.0 |
| Chloride ($Cl^-$) | IC | 0.0625 | 0.0210 | 0.1073 | 244 | 156 | 63.9 | 121 | 49.6 |
| Nitrate ($NO_3^-$) | IC | 0.0625 | 0.0208 | 0.0601 | 244 | 240 | 98.4 | 240 | 98.4 |
| Sulfate ($SO_4^=$) | IC | 0.0625 | 0.0214 | 0.2445 | 244 | 244 | 100.0 | 244 | 100.0 |
| Ammonium ($NH4^+$) | AC | 0.0625 | 0.0208 | 0.0208 | 244 | 241 | 98.8 | 243 | 99.6 |
| Soluble Sodium ($Na^+$) | AAS | 0.0098 | 0.0061 | 0.3532 | 244 | 244 | 100.0 | 138 | 56.6 |
| Soluble Potassium ($K^+$) | AAS | 0.0062 | 0.0021 | 0.0117 | 244 | 244 | 100.0 | 244 | 100.0 |
| **IMPROVE PROTOCOL** | | | | | | | | | |
| O1TC | TOR/TOT | 0.2246 | 0.0250 | 0.1556 | 244 | 182 | 74.6 | 198 | 81.1 |
| O2TC | TOR/TOT | 0.2246 | 0.0407 | 0.1819 | 244 | 239 | 98.0 | 240 | 98.4 |
| O3TC | TOR/TOT | 0.2246 | 0.1052 | 0.2284 | 244 | 235 | 96.3 | 235 | 96.3 |
| O4TC | TOR/TOT | 0.2246 | 0.0371 | 0.0791 | 244 | 236 | 96.7 | 243 | 99.6 |
| OPTTC | TOR/TOT | 0.2246 | 0.0275 | 0.0800 | 243 | 227 | 93.4 | 235 | 96.7 |
| OPTRC | TOR/TOT | 0.2246 | 0.0267 | 0.0000 | 244 | 125 | 51.2 | 160 | 65.6 |
| OCTTC | TOR/TOT | 0.2246 | 0.1525 | 0.5697 | 243 | 242 | 99.6 | 239 | 98.4 |
| OCTRC | TOR/TOT | 0.2246 | 0.1525 | 0.5271 | 244 | 243 | 99.6 | 240 | 98.4 |
| E1TC | TOR/TOT | 0.0300 | 0.0201 | 0.0476 | 244 | 244 | 100.0 | 244 | 100.0 |
| E2TC | TOR/TOT | 0.0300 | 0.0253 | 0.0668 | 244 | 242 | 99.2 | 237 | 97.1 |
| E3TC | TOR/TOT | 0.0300 | 0.0119 | 0.0384 | 244 | 5 | 2.0 | 4 | 1.6 |
| ECTTC | TOR/TOT | 0.0300 | 0.0318 | 0.0949 | 243 | 242 | 99.6 | 242 | 99.6 |
| ECTRC | TOR/TOT | 0.0300 | 0.0320 | 0.1166 | 244 | 244 | 100.0 | 244 | 100.0 |
| TCTC | TOR/TOT | 0.2246 | 0.1601 | 0.5824 | 244 | 244 | 100.0 | 243 | 99.6 |
| Sodium (Na) | XRF | 0.0397 | 0.0314 | 0.0898 | 244 | 244 | 100.0 | 238 | 97.5 |
| Magnesium (Mg) | XRF | 0.0144 | 0.0348 | 0.0427 | 244 | 232 | 95.1 | 201 | 82.4 |
| Aluminum (Al) | XRF | 0.0058 | 0.0235 | 0.0204 | 244 | 241 | 98.8 | 227 | 93.0 |
| Silicon (Si) | XRF | 0.0036 | 0.0108 | 0.0292 | 244 | 243 | 99.6 | 235 | 96.3 |
| Phosphorus (P) | XRF | 0.0032 | 0.0022 | 0.0042 | 244 | 244 | 100.0 | 244 | 100.0 |
| Sulfur (S) | XRF | 0.0029 | 0.0006 | 0.0055 | 244 | 244 | 100.0 | 244 | 100.0 |
| Chlorine (Cl) | XRF | 0.0058 | 0.0016 | 0.0047 | 244 | 206 | 84.4 | 211 | 86.5 |
| Patassium (K) | XRF | 0.0035 | 0.0001 | 0.0085 | 244 | 244 | 100.0 | 244 | 100.0 |
| Calcium (Ca) | XRF | 0.0026 | 0.0019 | 0.0037 | 244 | 244 | 100.0 | 244 | 100.0 |
| Titanium (Ti) | XRF | 0.0017 | 0.0011 | 0.0019 | 244 | 222 | 91.0 | 222 | 91.0 |
| Vanadium (V) | XRF | 0.0014 | 0.0004 | 0.0007 | 244 | 243 | 99.6 | 243 | 99.6 |
| Chromium (Cr) | XRF | 0.0011 | 0.0017 | 0.0013 | 244 | 132 | 54.1 | 121 | 49.6 |
| Manganese (Mn) | XRF | 0.0010 | 0.0050 | 0.0040 | 244 | 233 | 95.5 | 188 | 77.0 |
| Iron (Fe) | XRF | 0.0008 | 0.0074 | 0.0297 | 244 | 244 | 100.0 | 229 | 93.9 |
| Cobalt (Co) | XRF | 0.0005 | 0.0008 | 0.0015 | 244 | 24 | 9.8 | 3 | 1.2 |
| Nickel (Ni) | XRF | 0.0005 | 0.0013 | 0.0014 | 244 | 242 | 99.2 | 223 | 91.4 |
| Copper (Cu) | XRF | 0.0006 | 0.0010 | 0.0019 | 244 | 232 | 95.1 | 218 | 89.3 |
| Zinc (Zn) | XRF | 0.0006 | 0.0014 | 0.0056 | 244 | 244 | 100.0 | 236 | 96.7 |
| Gallium (Ga) | XRF | 0.0011 | 0.0043 | 0.0086 | 244 | 112 | 45.9 | 17 | 7.0 |
| Arsenic (As) | XRF | 0.0010 | 0.0011 | 0.0011 | 244 | 143 | 58.6 | 139 | 57.0 |
| Selenium (Se) | XRF | 0.0007 | 0.0010 | 0.0000 | 244 | 40 | 16.4 | 45 | 18.4 |

**Table 3-4.** (continued)

| Species | Analysis Method[a] | MDL[b] (µg/m$^3$) | RMS[c] (µg/m$^3$) | LQL[d] (µg/m$^3$) | No.of Values | No. > MDL | % > MDL | No. > LQL | % > LQL |
|---|---|---|---|---|---|---|---|---|---|
| Bromine (Br) | XRF | 0.0006 | 0.0011 | 0.0034 | 244 | 235 | 96.3 | 194 | 79.5 |
| Rubidium (Rb) | XRF | 0.0006 | 0.0010 | 0.0019 | 244 | 140 | 57.4 | 103 | 42.2 |
| Strontium (Sr) | XRF | 0.0006 | 0.0025 | 0.0034 | 244 | 135 | 55.3 | 20 | 8.2 |
| Yttrium (Y) | XRF | 0.0007 | 0.0016 | 0.0024 | 244 | 44 | 18.0 | 10 | 4.1 |
| Zerconium (Zr) | XRF | 0.0010 | 0.0034 | 0.0066 | 244 | 89 | 36.5 | 3 | 1.2 |
| Molybdenum (Mo) | XRF | 0.0016 | 0.0036 | 0.0051 | 244 | 89 | 36.5 | 8 | 3.3 |
| Palladium (Pd) | XRF | 0.0064 | 0.0048 | 0.0075 | 244 | 14 | 5.7 | 11 | 4.5 |
| Silver (Ag) | XRF | 0.0070 | 0.0037 | 0.0072 | 244 | 8 | 3.3 | 8 | 3.3 |
| Cadmium (Cd) | XRF | 0.0070 | 0.0041 | 0.0093 | 244 | 19 | 7.8 | 9 | 3.7 |
| Indium (In) | XRF | 0.0074 | 0.0040 | 0.0092 | 244 | 5 | 2.0 | 1 | 0.4 |
| Tin (Sn) | XRF | 0.0097 | 0.0048 | 0.0118 | 244 | 118 | 48.4 | 99 | 40.6 |
| Antimony (Sb) | XRF | 0.0103 | 0.0043 | 0.0160 | 244 | 19 | 7.8 | 3 | 1.2 |
| Barium (Ba) | XRF | 0.0299 | 0.0103 | 0.0207 | 244 | 6 | 2.5 | 16 | 6.6 |
| Lanthanum (La) | XRF | 0.0356 | 0.0214 | 0.0468 | 244 | 9 | 3.7 | 3 | 1.2 |
| Gold (Au) | XRF | 0.0018 | 0.0048 | 0.0086 | 244 | 20 | 8.2 | 1 | 0.4 |
| Mercury (Hg) | XRF | 0.0014 | 0.0018 | 0.0022 | 244 | 6 | 2.5 | 4 | 1.6 |
| Thallium (Tl) | XRF | 0.0014 | 0.0037 | 0.0050 | 244 | 9 | 3.7 | 1 | 0.4 |
| Lead (Pb) | XRF | 0.0017 | 0.0036 | 0.0044 | 244 | 223 | 91.4 | 204 | 83.6 |
| Uranium (U) | XRF | 0.0013 | 0.0047 | 0.0092 | 244 | 84 | 34.4 | 4 | 1.6 |

[a] IC=ion chromatography. AC=automated colorimetry. AAS=atomic absorption spectrophotometry. TOR= thermal/optical reflectance. XRF=x-ray fluorescence.

[b] Minimum detectable limit (MDL) is the concentration at which instrument response equals three times the standard deviation of the lab blanks concentrations. Typical sample volumes are 24.1 $m^3$.

[c] Root mean squared precision (RMS) is the square root of the sum of the squared uncertainties of the observations divided by the number of observations.

[d] Lower quantifiable limit (LQL) is three times the standard deviation of the field blank concentrations. LQL is expressed here in terms of mass per cubic meter after dividing by 24.1 $m^3$ for Partisol samplers.

These analytical specifications imply that $PM_{2.5}$ samples acquired during the study possess adequate sample loading for chemical analysis of those species that are expected from sources in the region. In addition, the MDLs of the selected chemical analysis methods were sufficiently low to establish valid measurements with acceptable precisions.

## 3.2 Quality Assurance

Quality control (QC) and quality auditing establish the precision, accuracy, and validity of measured values. Quality assurance integrates quality control, quality auditing, measurement method validation, and sample validation into the measurement process. The results of quality assurance are data values with specified precisions, accuracies, and validities.

QC is intended to prevent, identify, correct, and define the consequences of difficulties that might affect the precision and accuracy, and or validity of the measurements. Quality auditing consisted of systems and performance audits. The system audit should include a review of the operational and QC procedures to assess whether they were adequate for assuring valid data that met the specified levels of accuracy and precision. Quality auditing should also examine all phases of the measurement activity to determine that procedures were followed and that operators were properly trained. Performance audits should establish whether the predetermined specifications were achieved in practice. The performance audits should challenge the measurement/analysis systems with known transfer standards traceable to primary standards. Quality Control and Quality Auditing procedures were carried out by the HKEPD for the samplers and for filter mass analyses. Both system and performance audits were performed in DRI's Environmental Analysis Facility on an annual basis to assure data quality. Auditors acquired and reviewed the standard operating procedures and examined all phases of measurement activities to assure that procedures were followed and that operators were properly trained.

Field blanks were acquired and replicate analyses was performed for ~10% of all ambient samples. As previously mentioned, quality assurance audits of sample flow rates were conducted by the HKEPD throughout the study period. The audit results are not included in this report, but are available from the HKEPD. Data were submitted to two levels of data validation (Chow et al., 1994, Watson et al., 2001). Detailed data validation processes are documented in the following subsections.

## 3.3 Data Validation

Data acquired from the study were submitted to three data validation levels:

- Level 0 sample validation designates data as they come off the instrument. This process ascertains that the field or laboratory instrument is functioning properly.

- Level I sample validation: 1) flags samples when significant deviations from measurement assumptions have occurred, 2) verifies computer file entries against data sheets, 3) eliminates values for measurements that are known to be invalid because of instrument malfunctions, 4) replaces data from a backup data acquisition system in the event of failure of the primary system, and 5) adjusts values for quantifiable calibration or interference biases.

- Level II sample validation applies consistency tests to the assembled data based on known physical relationships between variables.

- Level III sample validation is part of the data interpretation process. The first assumption upon finding a measurement which is inconsistent with physical expectations, is that the unusual value is due to a measurement error. If, upon tracing the path of the measurement nothing unusual is found, the value can be assumed to be a valid result of an environmental cause. Unusual values are identified during the data interpretation process as: 1) extreme values, 2) values which would otherwise normally track the values of other variables in a time series, and 3) values for observables which would normally follow a qualitatively predictable spatial or temporal pattern.

Level I validation flags and comments are included with each data record in the database as documented in Section 3.1. Level II validation tests and results are described in the following subsections. Level III data validation will not be completed until further data analysis is performed.

Level II tests evaluate the chemical data for internal consistency. In this study, Level II data validations were made for: 1) sum of chemical species versus $PM_{2.5}$ mass, 2) physical consistency, 3) anion and cation balance, and 4) reconstructed versus measured mass. Correlations and linear regression statistics were computed and scatter plots prepared to examine the data.

### 3.3.1 Sum of Chemical Species versus Mass

The sum of the individual chemical concentrations for $PM_{2.5}$ should be less than or equal to the corresponding gravimetrically measured mass concentrations. This sum includes chemicals quantified on the Teflon-membrane and quartz-fiber filters. Total sulfur (S), soluble chloride ($Cl^-$), and soluble potassium ($K^+$) are excluded from the sum to avoid double counting, since sulfate ($SO_4^=$), chlorine (Cl), and total potassium (K) are included in the sum. Elemental sodium (Na) and magnesium (Mg) have low atomic numbers and require detailed particle size distributions in order to completely correct for particle x-ray absorption effects, so these concentrations are also excluded from the calculation. Measured concentrations do not account for unmeasured metal oxides in crustal material, unmeasured cations, or hydrogen and oxygen associated with organic carbon.

Statistical analysis reported in each plot included in this report includes simple linear regression models whereby error is assumed in the response variate (*y*-axis), and no error is assumed for the explanatory variate (*x*-axis). Residuals of regression are assumed independent identically distributed normal with mean zero and constant variance. Analysis of variance tables were constructed to check for significance of regression on each model. While F-Ratios indicated significance in regression for all models included in this report, there were some intercept parameters which did test zero, and all regression parameters were checked at the 5% level of significance. Those regression models without significant intercept parameters were rerun to include only the slope parameter, and all corresponding calculations to the new models were recalculated including correlation and standard error of the parameter estimate. Additional information includes the biased mean of the ratios $Y/X$ and the standard error of the biased mean.

Figure 3-2 shows scatter plots of the $PM_{2.5}$ sum of species versus mass on Teflon filters for all the sites combined and for each of the individual sites. Each plot contains a

a) All sites

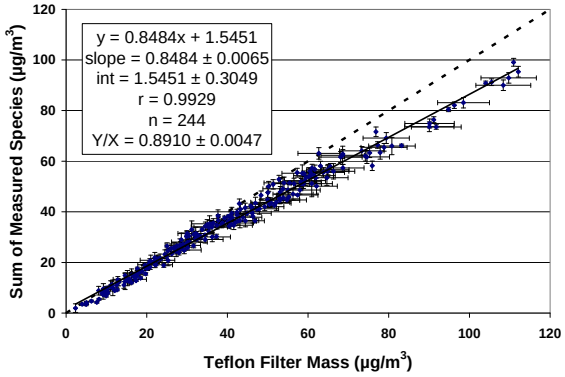


b) Mong Kok (MK)

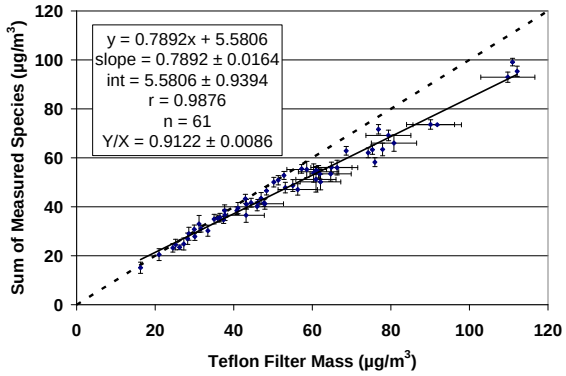


c) Tsuen Wan (TW)

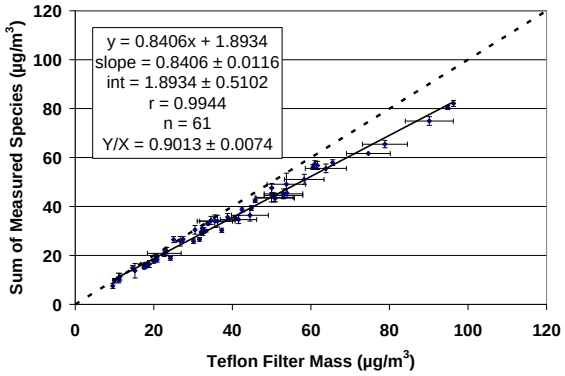


d) Hok Tsui (HT)

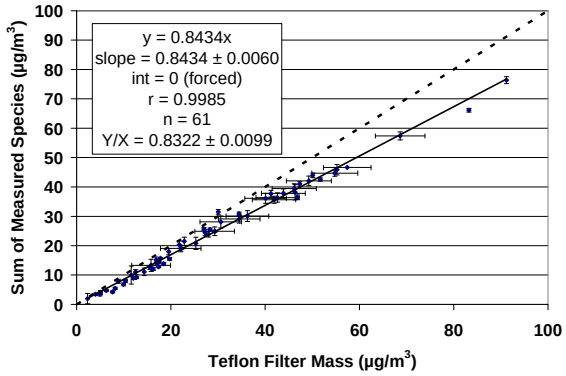


e) Yuen Long (YL)

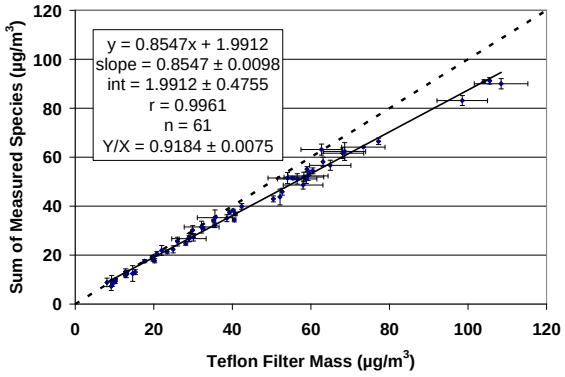


**Figure 3-2.** Scatter plots of sum of species versus mass measurements from $PM_{2.5}$ data acquired at: a) all four sites; b) the MK site; c) the TW site; d), the HT site; and e) the YL site.

solid line indicating the slope with intercept and a dashed one-to-one line. Measurement uncertainties associated with the x- and y-axes are shown for comparison. Regression statistics with mass as the independent variable (X) and sum of species as the dependent variable (Y) are also calculated. The calculated correlation coefficient and number of data points is also shown for comparison, as is the average of the ratios of Y over X. As intercepts are low compared to the measured concentrations, the slope closely represents the ratio of Y over X. Any suspect data were examined, flagged, and removed if applicable from statistical analysis when sampling or analytical anomalies were identified.

As shown by Figure 3-2a, all of the sums are less than the corresponding $PM_{2.5}$ mass within the reported precisions. An excellent relationship was found between the sum of species and mass, with correlation coefficients exceeding 0.98 for the all measurements. Approximately 85% of the $PM_{2.5}$ mass was explained by the chemical species measured during the study.

Comparisons among the individual sites were similar. Figures 3-2b, c, d, and e show that all $PM_{2.5}$ measurements are below the one-to-one line within measurement uncertainties. High correlations (r=>0.99) are also seen for all of the sites. These comparisons are also very similar, with the exception of the HT background site which exhibited somewhat lower mass concentrations. The intercept coefficient for the HT background site is much closer to zero than the intercept for the other two sites. Since organic carbon is often a large portion of $PM_{2.5}$ mass, the elevated sum of species was affected by high carbon mass at the MK, TW and YL sites.

### 3.3.2 Physical Consistency

The composition of chemical species concentrations measured by different chemical analysis methods was examined. Physical consistency was tested for: 1) sulfate versus total sulfur, 2) chloride versus chlorine, and 3) soluble potassium versus total potassium.

#### 3.3.2.a Sulfate versus Total Sulfur

Water-soluble sulfate ($SO_4^{=}$) was measured by ion chromatography (IC) analysis on quartz-fiber filters, and total sulfur (S) was measured by x-ray fluorescence (XRF) analysis on Teflon-membrane filters. The ratio of sulfate to total sulfur should equal "3" if all of the sulfur were present as soluble sulfate. Figure 3-3a shows scatter plots of sulfate versus sulfur concentrations for all three sites. A good correlation (r>0.96) was found among $PM_{2.5}$ sulfur/sulfate measurements with an average ratio of 3.35±0.24.

High correlations (r>0.98) were found for $PM_{2.5}$ sulfate/sulfur comparisons among the individual sites. Figures 3-3b, c, d and e show that all but a few of the data pairs fell beyond the three-to-one line. The regression statistics give a slope ranging from 3.06±0.05 to 3.71±0.13 The slopes for each site are being pulled high by the samples taken on 9/11/2005 and 10/17/2005. These two days exhibited very high mass concentrations (typically greater than 100 $\mu g/m^3$), however the field and analytical data were verified and are valid. With such heavily loaded filters it is possible that x-ray attenuation may have resulted in lower than expected sulfur concentrations as measured by the EDXRF. Overall, the sulfate and total sulfur comparisons in this study support the contentions that nearly all sulfur was present as soluble sulfate in the atmosphere and that both XRF and IC measurements are valid.

a) All sites

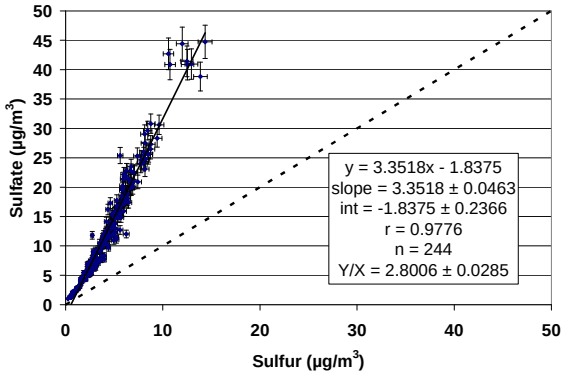


b) Mong Kok (MK)

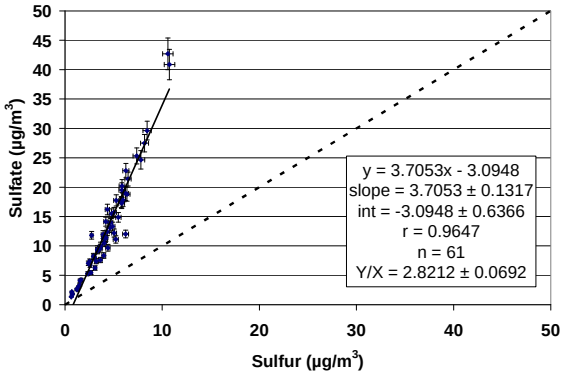


c) Tsuen Wan (TW)

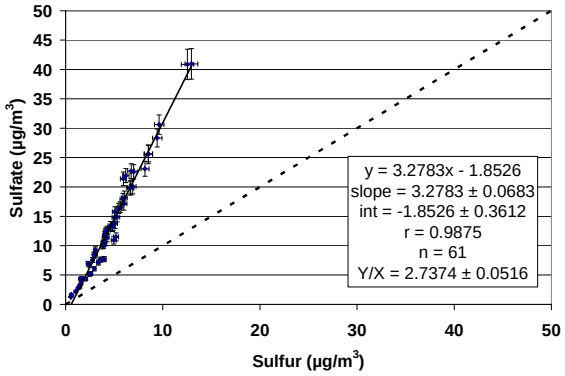


d) Hok Tsui (HT)

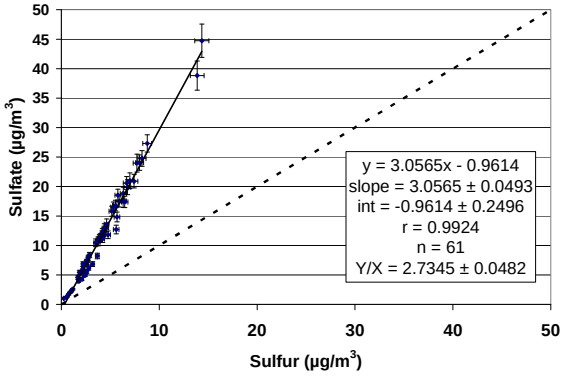


e) Yuen Long (YL)

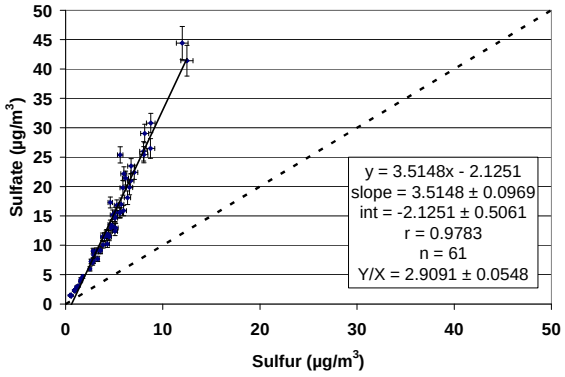


**Figure 3-3.** Scatter plots of sulfate versus sulfur measurements from $PM_{2.5}$ data acquired at: a) all four sites; b) the MK site; c) the TW site; d) the HT site; and e) the YL site.

### 3.3.2.b Chloride versus Chlorine

Chloride ($Cl^-$) was measured by IC on quartz-fiber filters, and chlorine (Cl) was measured by XRF on Teflon-membrane filters. Because chloride is the water-soluble portion of chlorine, the chloride-to-chlorine ratio is expected to be less than unity. Figure 3-4a shows that moderate correlations (r=0.90) were found between $PM_{2.5}$ chloride and chlorine measurements, with a slope close to unity and low intercepts for all of the sites. The uncertainties of chloride measurements were higher at low concentrations because chloride's elution peak in ion chromatographic analysis is close to the distilled water dip which, in turn, shifts the baseline of the chromatogram (Chow and Watson, 1999). In addition, chlorine collected on the Teflon filter may be lost through volatilization, because XRF analysis is conducted in a vacuum chamber. Such losses are especially apparent when chlorine concentrations are low.

a) All sites

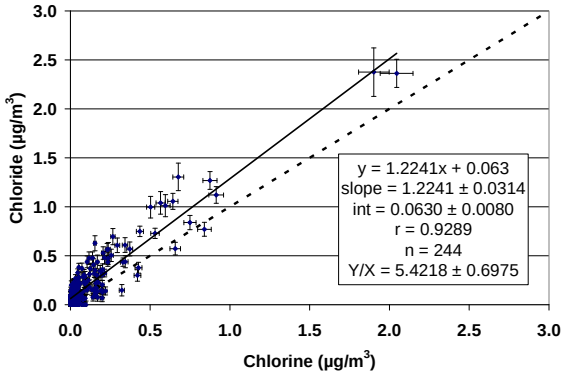


b) Mong Kok (MK)

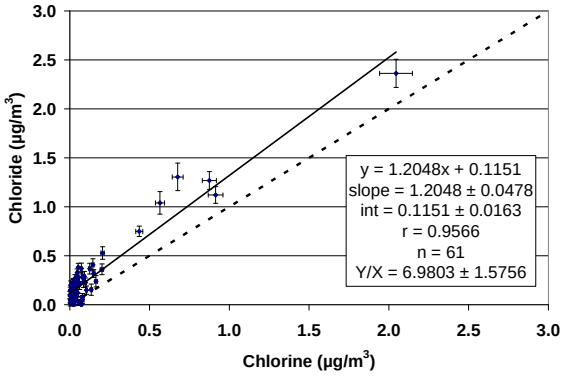


c) Tsuen Wan (TW)

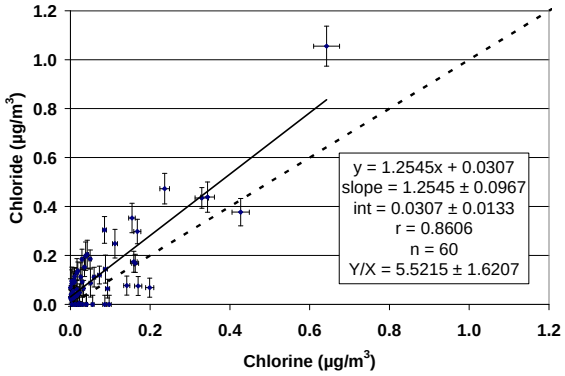


d) Hok Tsui (HT)

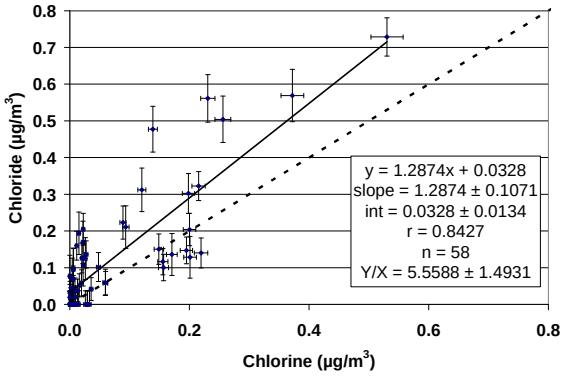


e) Yuen Long (YL)

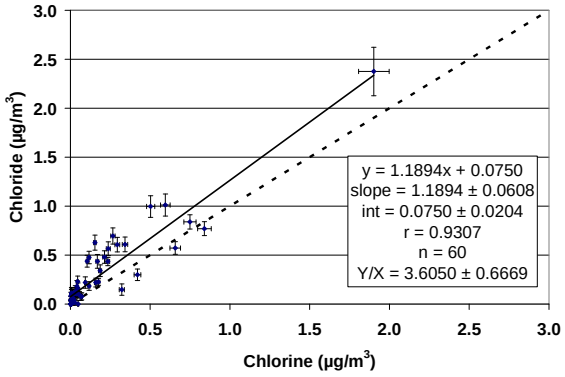


**Figure 3-4.** Scatter plots of chloride versus chlorine measurements from $PM_{2.5}$ data acquired at: a) all four sites; b) the MK site; c) the TW site; d) the HT site; and e) the YL site.

### 3.3.2.c Soluble Potassium versus Total Potassium

Soluble potassium ($K^+$) was acquired by atomic absorption spectrophotometry (AAS) analysis on quartz-fiber filters, and total potassium (K) was acquired by XRF analysis on Teflon-membrane filters. Since potassium concentrations are often used as an indicator of vegetative burning, it is important to assure the validity of the $K^+$ measurement.

Figure 3-5 displays the scatter plots of soluble potassium versus total potassium concentrations. This analysis shows that $K^+$ concentrations are low to moderate throughout the study area, even though an average of 90% of the total potassium is in its soluble state. The average y/x ratio of $K^+/K$ was 0.91±0.01. The higher $K^+/K$ ratios imply that vegetative burning or long-range transport of wildfire emissions are prominent in the study area.

a) All sites

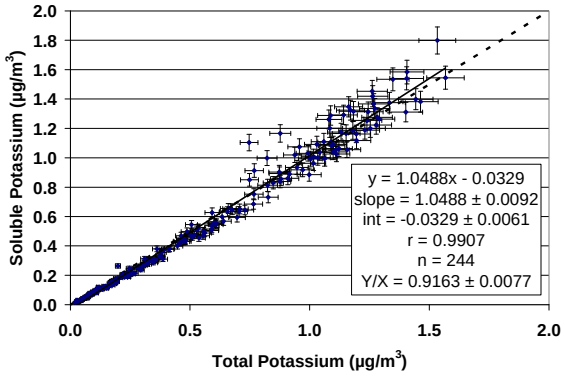


b) Mong Kok (MK)

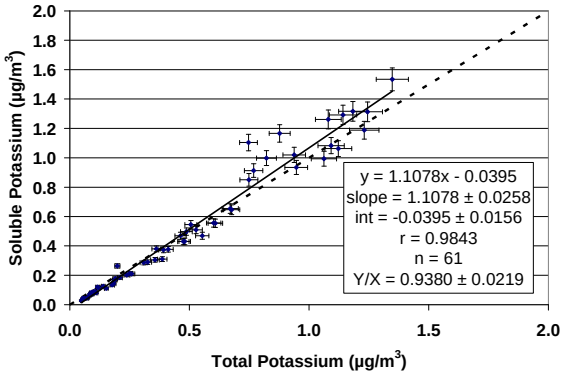


c) Tsuen Wan (TW)

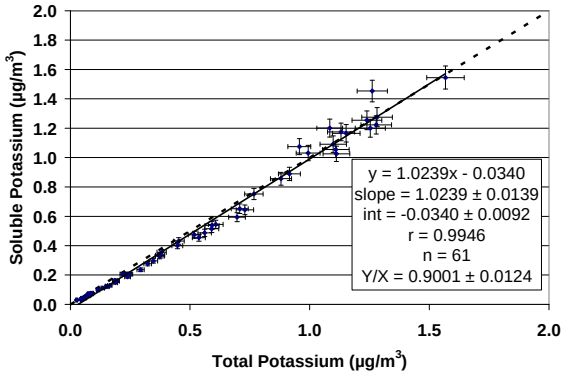


d) Hok Tsui (HT)

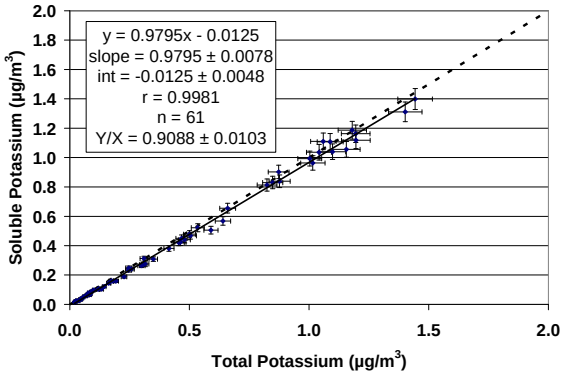


e) Yuen Long (YL)

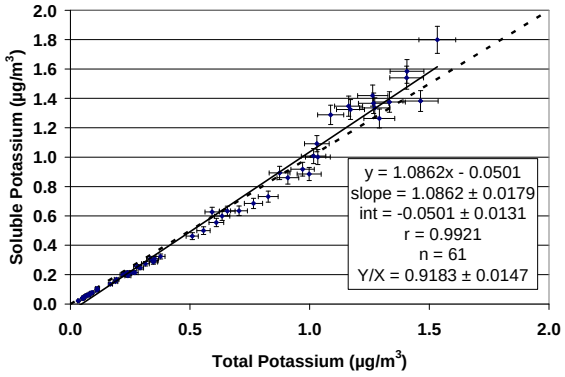


**Figure 3-5.** Scatter plots of soluble potassium versus total potassium measurements from $PM_{2.5}$ data acquired at: a) all four sites; b) the MK site; c) the TW site; d) the HT site; and e) the YL site.

### 3.3.2.d Ammonium Balance

Ammonium nitrate ($NH_4NO_3$), ammonium sulfate ($[NH_4]_2SO_4$), and ammonium bisulfate ($NH_4HSO_4$), are the most likely nitrate and sulfate compounds to be found in Hong Kong. Some sodium nitrate ($NaNO_3$) and/or sodium sulfate ($Na_2SO_4$) may also be present at the coastal sites, which may be attributable to transport by prevailing winds from the Pacific Ocean into Hong Kong, especially during summer. Ammonium ($NH_4^+$) can be calculated based on the stoichiometric ratios of the different compounds and compared with that which was measured. In Figure 3-6, ammonium is calculated from nitrate and sulfate, assuming that all nitrate was in the form of ammonium nitrate and all sulfate was in the form of either ammonium sulfate (i.e., calculated ammonium = [0.38 × sulfate] + [0.29 × nitrate]) or ammonium bisulfate (i.e., ammonium = [0.192 × sulfate] + [0.29 × nitrate]). These calculated values were compared with the measured values for ammonium.

a) All sites

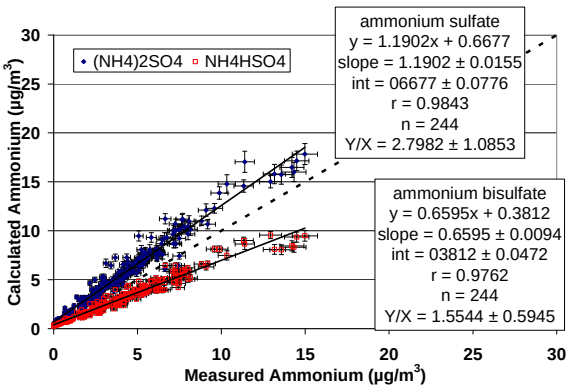


b) Mong Kok (MK)

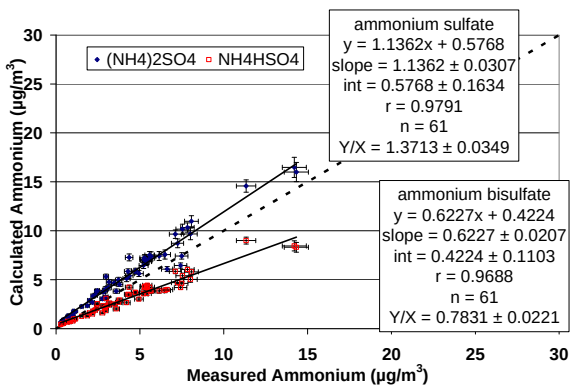


c) Tsuen Wan (TW)

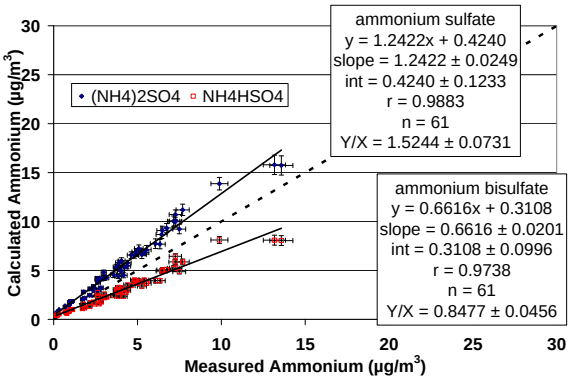


d) Hok Tsui (HT)

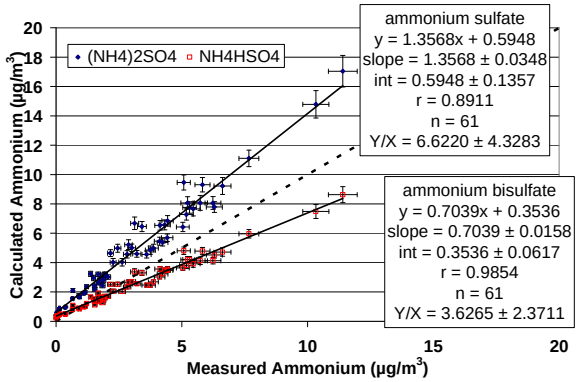


e) Yuen Long (YL)

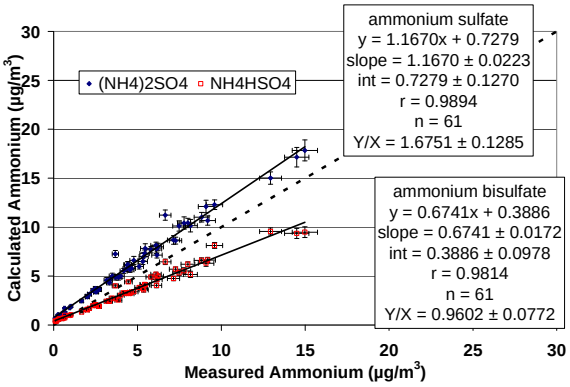


**Figure 3-6.** Scatter plots of calculated ammonium versus measured ammonium from $PM_{2.5}$ data acquired at: a) all four sites; b) the MK site; c) the TW site; d) the HT site and e) the YL site.

With a few exceptions during the study period, Figure 3-6 shows excellent agreement for $PM_{2.5}$ ammonium with a correlation coefficients exceeding 0.97 when ammonium sulfate or ammonium bisulfate was assumed. However, the slopes seen in these figures average 1.19±0.02 assuming ammonium sulfate, and 0.66±0.01 assuming ammonium bisulfate. These data thus imply that a majority of the sulfate was neutralized and in the form of ammonium sulfate during the study period.

When all sulfate and nitrate are assumed to be fully neutralized, calculated ammonium exceeds measured ammonium. This phenomenon typically is more pronounced in the $PM_{10}$ fraction than in the $PM_{2.5}$ fraction, indicating the presence of coarse-particle sulfate and/or nitrate salts that might be associated with water-soluble $Ca^{++}$ or $Na^{+}$ ions. The chromatograms from ion chromatography analysis for nitrate and sulfate and graphs from automated colorimetry analysis for ammonium were examined, but no anomalies were found.

### 3.3.3 Anion and Cation Balance

The anion and cation balance in Figure 3-7 also shows a slight deficiency in cations that is not accounted for by measured anions. The correlations are high ($r>0.98$) in the $PM_{2.5}$ size fraction. The difference may be attributable to unmeasured $H^{+}$. The difference could also be due to the presence of coarse-particle sulfate and/or nitrate salts in a form other than ammonium sulfate and/or ammonium nitrate. However, Figure 3-7 generally indicates a close balance between anions and cations.

a) All sites

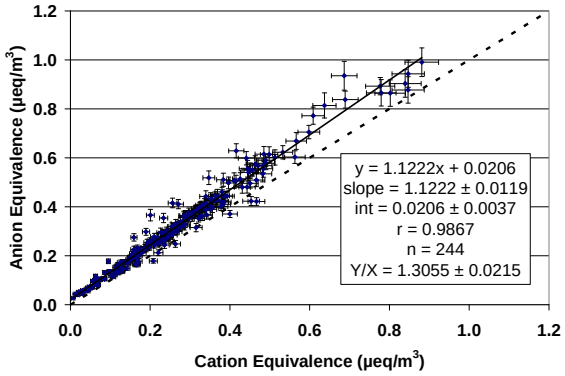


b) Mong Kok (MK)

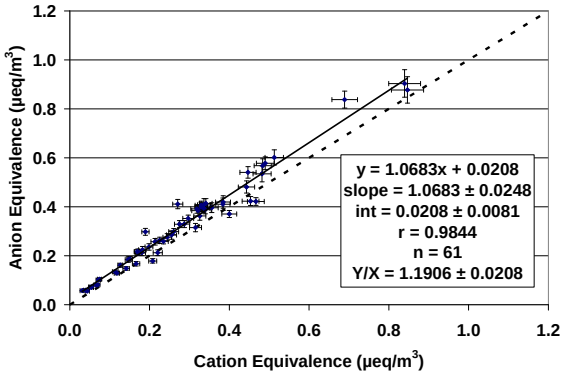


c) Tsuen Wan (TW)

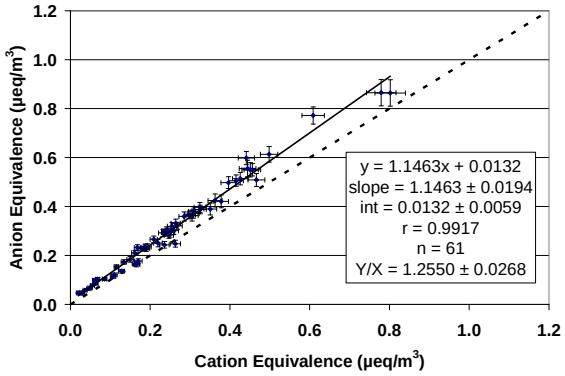


d) Hok Tsui (HT)

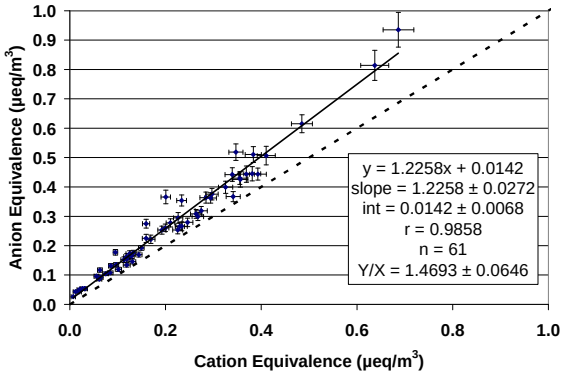


e) Yuen Long (YL)

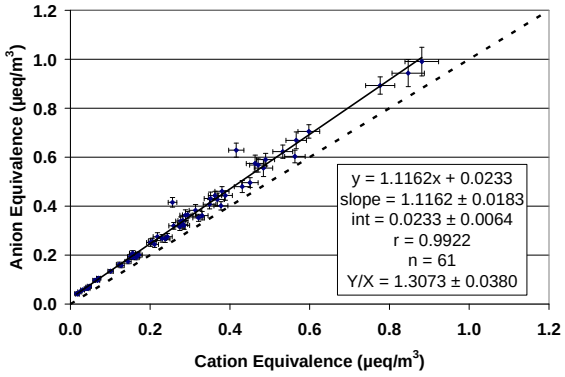


**Figure 3-7.** Scatter plots of cation versus anion measurements from $PM_{2.5}$ data acquired at: a) all four sites; b) the MK site; c) the TW site; d) the HT site; and e) the YL site.

### 3.3.4 IMPROVE Protocol Reflectance versus Transmittance for Organic and Elemental Carbon Measurements

Organic carbon (OC), and EC determined by IMPROVE TOR and TOT methods for samples from each site and all sites combined are compared in Figure 3-8 and 3-9. Laser reflectance and transmittance represent two different ways of determining the OC/EC split, as described in Section 2.2.

At all sites the correlation between organic carbon determined by laser reflectance versus transmittance exceeded $r = 0.97$. Elemental carbon also exhibited good correlation with $r > 0.91$.

a) All sites

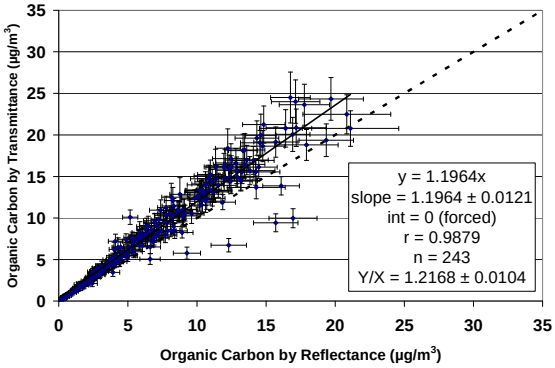


b) Mong Kok (MK)

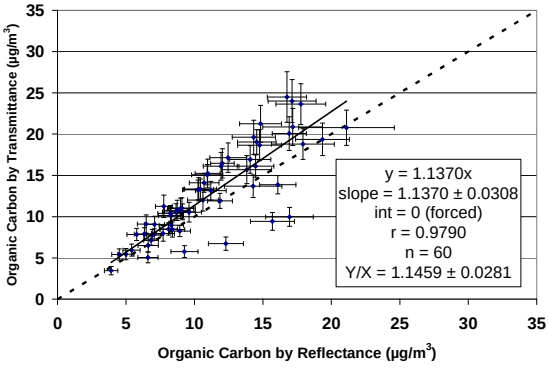


c) Tsuen Wan (TW)

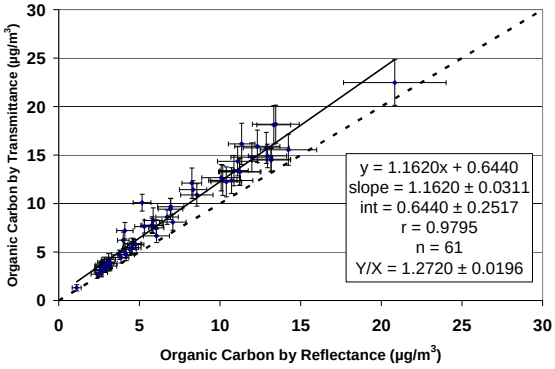


d) Hok Tsui (HT)

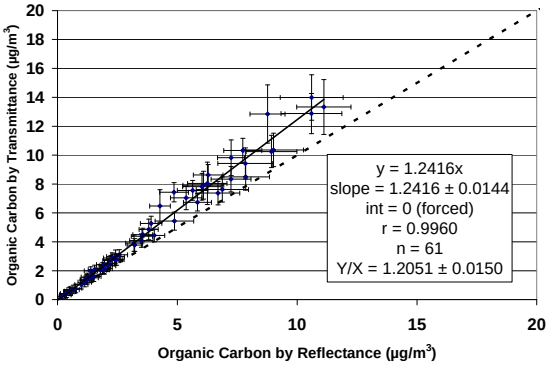


e) Yuen Long (YL)

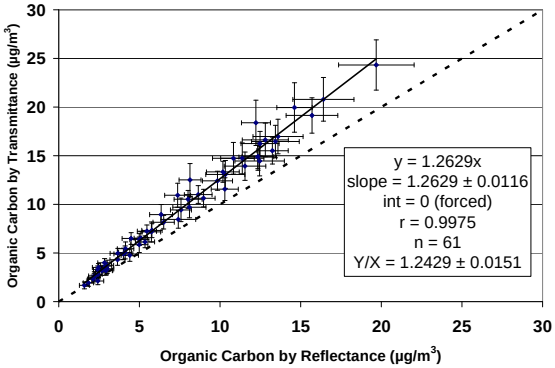


**Figure 3-8.** Comparisons of $PM_{2.5}$ OC by transmittance versus reflectance at: a) all four sites, b) the MK site, c) the TW site, d) the HT site, and e) the YL site.

a) All sites

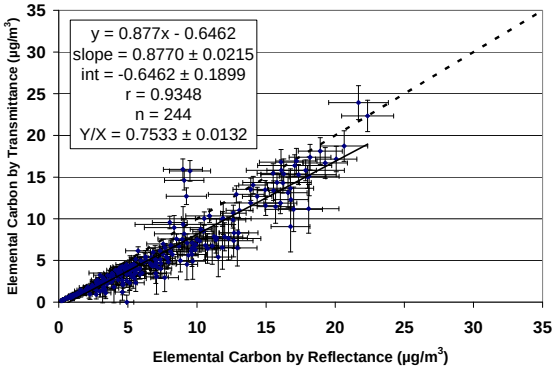


b) Mong Kok (MK)

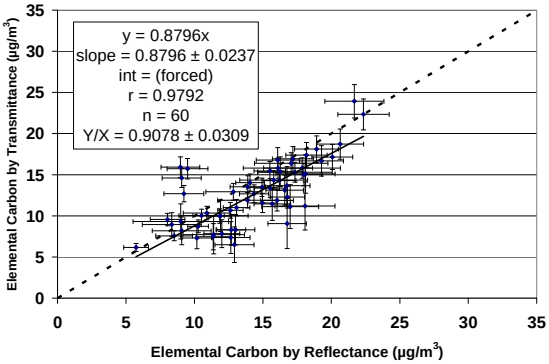


c) Tsuen Wan (TW)

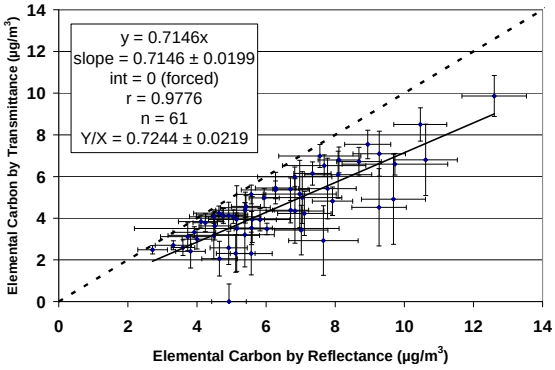


d) Hok Tsui (HT)

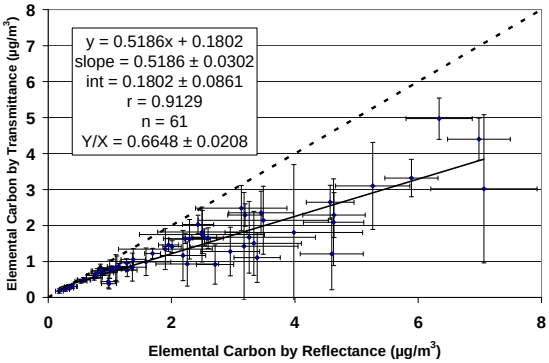


e) Yuen Long (YL)

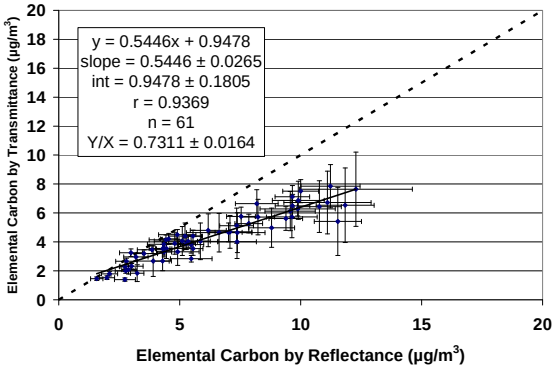


**Figure 3-9.** Comparisons of $PM_{2.5}$ EC by transmittance versus reflectance at: a) all four sites, b) the MK site, c) the TW site, d) the HT site, and e) the YL site.

### 3.3.5 Reconstructed versus Measured Mass

Major PM components can be used to reconstruct PM mass. The major components include: 1) geological material (estimated as 1.89×Al + 2.14×Si + 1.4×Ca + 1.43×Fe to account for unmeasured oxides), 2) organic matter (OM: 1.4×OC to account for unmeasured hydrogen and oxygen), 3) soot (elemental carbon), 4) ammonium sulfate, 5) ammonium nitrate, and 6) noncrustal trace elements (sum of other-than-geological trace elements). The difference between the constructed mass and the measured mass is referred to as unidentified mass.

The reconstructed mass are highly correlated to the measured mass at $r^2 \sim 0.98$ at all sites (Figure 3-10). In contrast to the sum-of-species-versus-mass comparison in Figure 3-2, unaccounted mass is largely eliminated when unmeasured oxygen and hydrogen were factored in. This confirms the validity of gravimetric and chemical measurements.

a) All sites

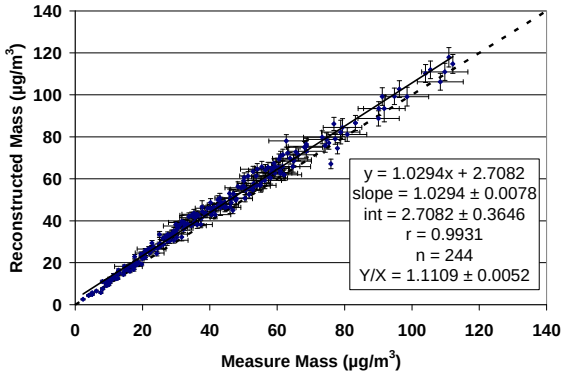


b) Mong Kok (MK)

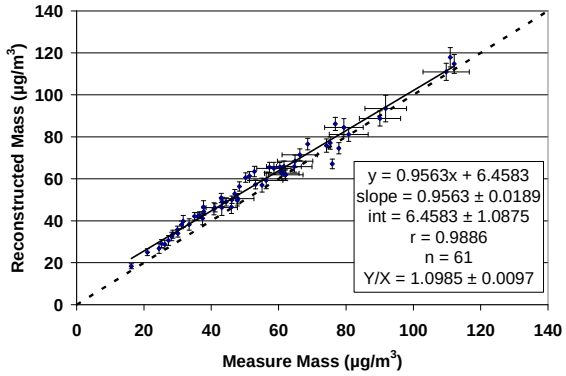


c) Tsuen Wan (TW)

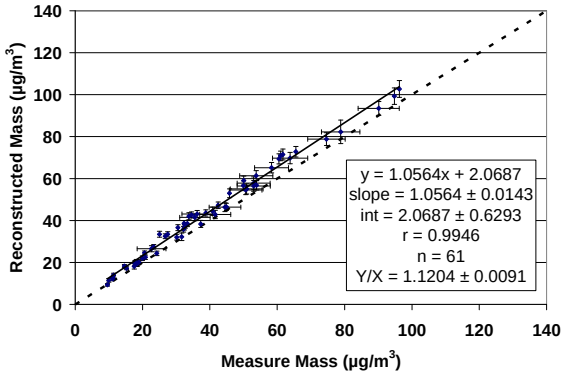


d) Hok Tsui (HT)

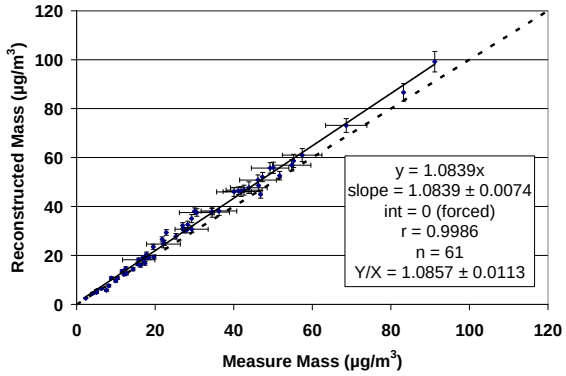


e) Yuen Long (YL)

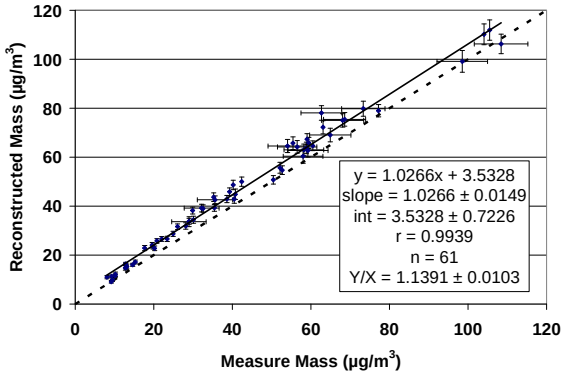


**Figure 3-10.** Scatter plots of reconstructed mass versus measured mass from $PM_{2.5}$ data acquired at: a) all four sites; b) the MK site; c) the TW site; d) the HT site; and e) the YL site.

Figure 3-11 shows the annual average composition (%) of these major components to $PM_{2.5}$ mass. The unidentified mass was set to zero when the reconstructed mass is greater than the measured mass (i.e. unidentified mass is negative), and the mass fractions of the major components were adjusted accordingly. This occurred only at all sites with unidentified mass ~ -4% of measured mass; this could be due to overestimation of some species, such as organic matter. Overall, the reconstructed mass agrees with the measured mass within ~5 %.

a) All sites

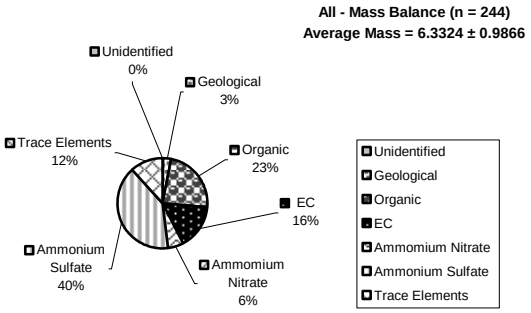


b) Mong Kok (MK)

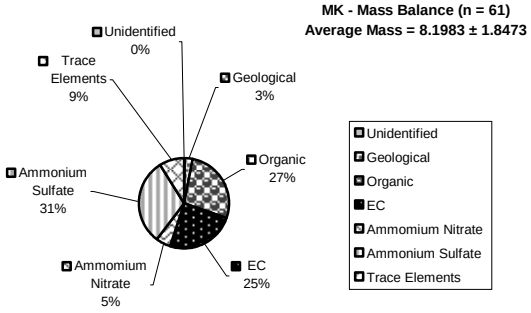


c) Tsuen Wan (TW)

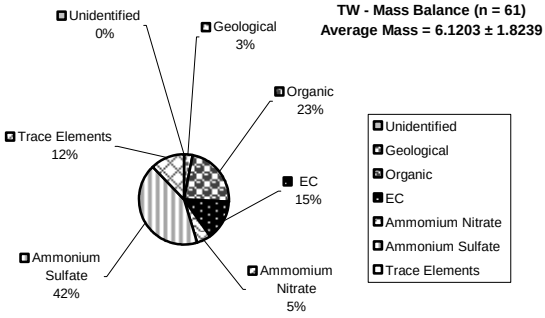


d) Hok Tsui (HT)

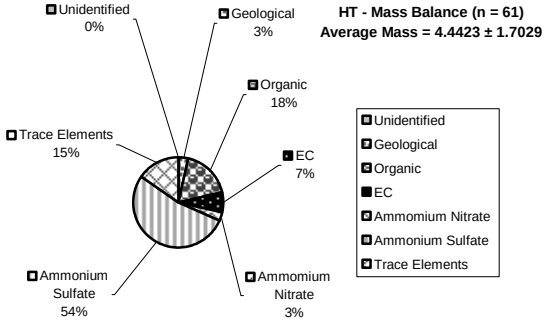


e) Yuen Long (YL)

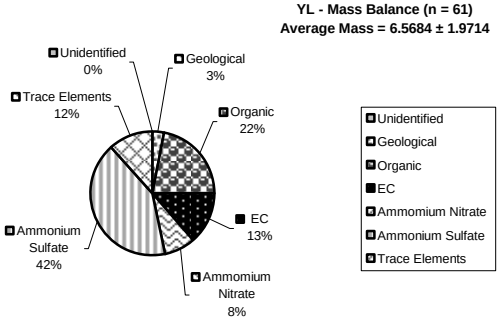

**Figure 3-11.** Material balance charts for $PM_{2.5}$ data acquired at: a) the four sites; b) the MK site; c) the TW site; d) the HT site; and e) the YL site. The major components of reconstructed mass include: 1) geological material (estimated as 1.89×Al + 2.14×Si + 1.4×Ca + 1.43×Fe to account for unmeasured oxides), 2) organic matter (1.4×organic carbon to account for unmeasured hydrogen and oxygen), 3) soot (elemental carbon), 4) ammonium sulfate, 5) ammonium nitrate, 6) noncrustal trace elements (sum of other-than-geological elements listed in Table 3-4 excluding Al, Si, Ca, Fe, Cl, and S), and 7) unidentified mass (difference between measured mass and the sum of the major components).

Figure 3-12 demonstrates the categorical cumulative totals for the 25%tile, 50%tile and 75%tile of reconstructed mass $PM_{2.5}$ days at the four sites. On high $PM_{2.5}$ days, the increased mass consists mostly of ammoniated sulfate and OM, both of which can be of secondary origin. High sulfate and OM concentrations usually occurred simultaneously across all four sites, suggesting the presence of variable regional sources. The change in EC concentration, a primary combustion tracer, is relatively limited at MK and TW. Nearby traffic emissions provide a consistent source for EC at the urban sites. The HT site does not have significant sources nearby, so most of the pollutants measured at this site were probably transported from distant urban areas.

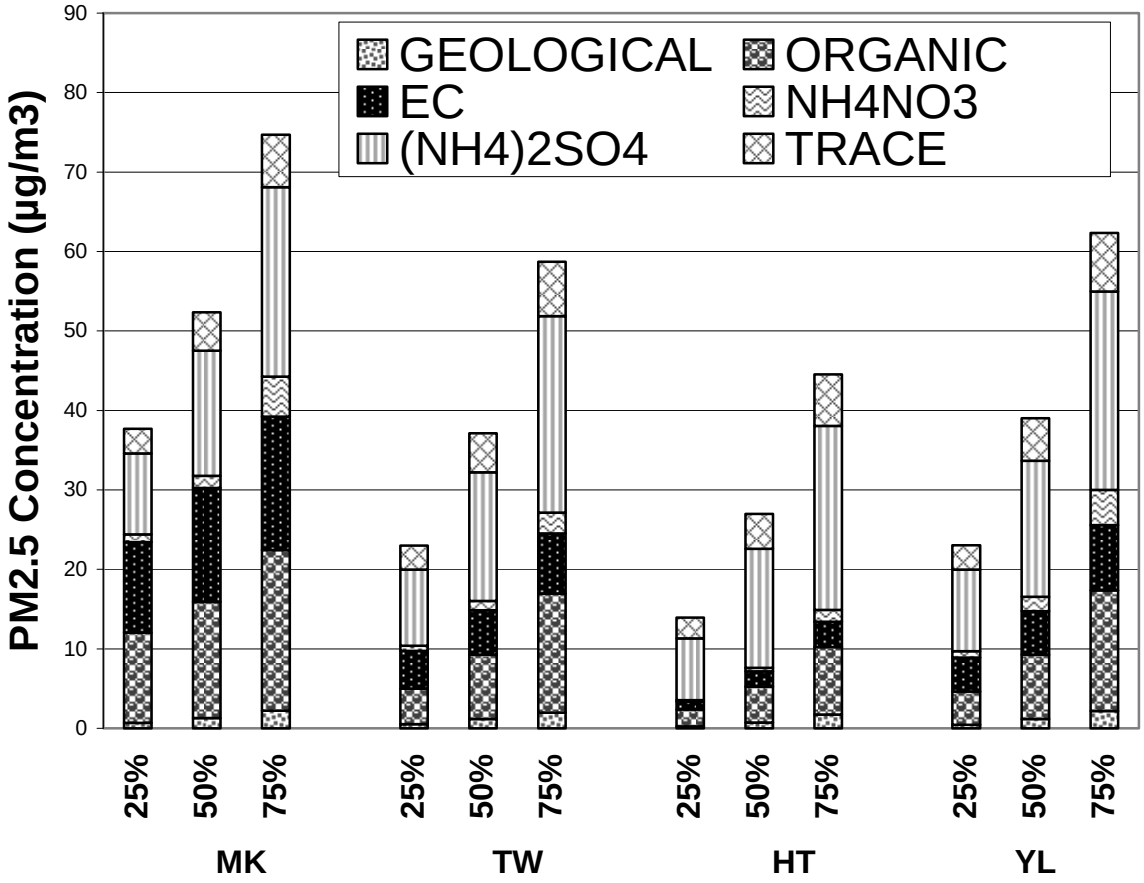


**Figure 3-12.** Mean reconstructed mass and chemical composition the 25%tile, 50-%tile and 75-%tile $PM_{2.5}$ days at the Mong Kok (MK), Hok Tsui (HT), Tsuen Wan (TW), and Yuen Long (YL) sites.

# 4. COMPARISON TO FIRST YEAR STUDY

Table 4-1 shows the side-by-side comparison of the first year study of samples collected during 2000-2001 and the current 2004 -2005 study. An additional site (Yuen Long [YL]) was added during this study, so no comparisons can be made for it; but the average concentration data from the YL site are presented for completeness. Mass concentrations show a significant increase at the Hok Tsui (HT, 16.8%) and Tsuen Wan (TW, 11.6%) sites, while the Mong Kok (MK) site exhibited a decrease of -9.9%.

Nitrate, sulfate and ammonium concentrations trended upward from the first year study until now. Sulfate and ammonium showed nearly the exact same rate of increase, and total sulfur by XRF shows essentially the same level of increase as the sulfate by ion chromatography, thereby increasing the confidence in the validity of all three chemical measurements. These secondary pollutants are often used as indicators to assess the influence from pollution in a regional basis. Their increase over the territory indicates the deterioration in the regional air quality.

Several other elemental concentrations show what appear to be significant changes (e.g., a nearly 100% increase in measured phosphorous concentrations). However, the increase or decrease in micrograms per cubic meter concentrations are actually quite small. It should also be noted that the first year study filters were analyzed on an older model Kevex energy dispersive XRF machine which was replaced with a new system prior to the analysis of the current study filter samples. The new system is a PanAlytical Epsilon 5 energy dispersive XRF system. While both systems operate under the same basic analysis principles, both the hardware and software have been upgraded with the new system.

Organic and elemental carbon both showed a significant decrease in concentration (-49% and -44% respectively) at the MK site. The reduction in carbon levels at the roadside site suggests the significant contributions from the programs about reduction in vehicular emissions, tightening diesel fuel and vehicle emission standards, over these years. Whereas the other two sites, HT and TW, showed decreased organic carbon with a corresponding increase in elemental carbon.

**Table 4-1.** Side-by-side comparison of the first year study of samples collected during 2000-2001 and the current 2004 -2005 study.

| Year 2000-2001 Study | HT | MK | TW | Year 2004-2005 Study | HT | MK | TW | YL | **Percent Difference** | **Percent Difference** | **Percent Difference** |
|---|---|---|---|---|---|---|---|---|---|---|---|
| Average Teflon Mass | 23.6575 | 58.2806 | 34.1221 | Average Teflon Mass | 28.4374 | 53.0228 | 38.5926 | 41.3102 | 16.81 | -9.92 | 11.58 |
| Average Quartz Mass | 25.8475 | 62.5022 | 37.2802 | Average Quartz Mass | 29.6432 | 54.8681 | 40.7482 | 43.9080 | 12.80 | -13.91 | 8.51 |
| Average of $Cl^-$ | 0.1428 | 0.2555 | 0.1376 | Average of $Cl^-$ | 0.1241 | 0.2827 | 0.1257 | 0.2642 | -15.06 | 9.63 | -9.40 |
| Average of NO3- | 0.7079 | 1.6527 | 1.3426 | Average of NO3- | 0.7619 | 2.4040 | 1.6350 | 2.8642 | 7.09 | 31.25 | 17.88 |
| Average of SO4= | 8.6410 | 9.5022 | 9.1721 | Average of SO4= | 11.9062 | 12.8397 | 13.1737 | 13.9100 | 27.42 | 25.99 | 30.38 |
| Average of NH4+ | 2.1570 | 3.1739 | 2.9645 | Average of NH4+ | 3.0590 | 4.4003 | 4.0702 | 4.6173 | 29.49 | 27.87 | 27.17 |
| Average of Na+ | 0.6794 | 0.3978 | 0.3972 | Average of Na+ | 0.5265 | 0.4228 | 0.3624 | 0.3745 | -29.04 | 5.92 | -9.59 |
| Average of K+ | 0.4026 | 0.4567 | 0.4921 | Average of K+ | 0.4333 | 0.4787 | 0.4862 | 0.5615 | 7.08 | 4.60 | -1.21 |
| Average of OC | 4.2256 | 16.6419 | 8.6898 | Average of OC | 3.9213 | 11.1770 | 6.9317 | 7.2348 | -7.76 | -48.89 | -25.36 |
| Average of EC | 1.6824 | 20.2884 | 5.3705 | Average of EC | 2.2770 | 14.1154 | 6.2578 | 6.1939 | 26.11 | -43.73 | 14.18 |
| Average of TC | 5.8897 | 36.9105 | 14.0405 | Average of TC | 6.1899 | 25.2839 | 13.1811 | 13.4203 | 4.85 | -45.98 | -6.52 |
| Average of Al | 0.1091 | 0.1139 | 0.1146 | Average of Al | 0.1223 | 0.1408 | 0.1414 | 0.1448 | 10.84 | 19.11 | 18.97 |
| Average of Si | 0.3489 | 0.4778 | 0.3870 | Average of Si | 0.2546 | 0.3469 | 0.3141 | 0.3221 | -37.00 | -37.76 | -23.22 |
| Average of Ph | 0.0028 | 0.0092 | 0.0050 | Average of Ph | 0.1747 | 0.1886 | 0.1950 | 0.1917 | 98.39 | 95.14 | 97.44 |
| Average of Su | 3.0534 | 3.4886 | 3.3789 | Average of Su | 4.2099 | 4.3005 | 4.5835 | 4.5622 | 27.47 | 18.88 | 26.28 |
| Average of Cl | 0.1432 | 0.1169 | 0.0874 | Average of Cl | 0.0709 | 0.1391 | 0.0758 | 0.1590 | -101.94 | 15.98 | -15.39 |
| Average of K | 0.4892 | 0.5517 | 0.5858 | Average of K | 0.4551 | 0.4678 | 0.5080 | 0.5631 | -7.49 | -17.93 | -15.32 |
| Average of Ca | 0.1024 | 0.1705 | 0.1262 | Average of Ca | 0.0652 | 0.1082 | 0.0896 | 0.0891 | -57.04 | -57.65 | -40.81 |
| Average of Ti | 0.0079 | 0.0092 | 0.0088 | Average of Ti | 0.0062 | 0.0109 | 0.0102 | 0.0114 | -27.81 | 15.26 | 13.59 |
| Average of V | 0.0117 | 0.0134 | 0.0137 | Average of V | 0.0167 | 0.0190 | 0.0237 | 0.0195 | 30.07 | 29.40 | 41.97 |
| Average of Cr | 0.0006 | 0.0010 | 0.0009 | Average of Cr | 0.0014 | 0.0017 | 0.0015 | 0.0017 | 53.00 | 38.91 | 39.58 |
| Average of Mn | 0.0077 | 0.0128 | 0.0124 | Average of Mn | 0.0123 | 0.0170 | 0.0158 | 0.0170 | 37.08 | 24.73 | 21.60 |
| Average of Fe | 0.1219 | 0.2692 | 0.1871 | Average of Fe | 0.1190 | 0.2579 | 0.1858 | 0.1996 | -2.41 | -4.38 | -0.71 |
| Average of Co | 0.0002 | 0.0001 | 0.0001 | Average of Co | 0.0002 | 0.0001 | 0.0001 | 0.0001 | -19.82 | -130.64 | -110.34 |
| Average of Ni | 0.0047 | 0.0055 | 0.0054 | Average of Ni | 0.0050 | 0.0061 | 0.0071 | 0.0068 | 5.71 | 8.91 | 24.30 |
| Average of Cu | 0.0052 | 0.0113 | 0.0090 | Average of Cu | 0.0065 | 0.0110 | 0.0104 | 0.0113 | 20.14 | -2.97 | 13.89 |
| Average of Zn | 0.1087 | 0.1794 | 0.1743 | Average of Zn | 0.1727 | 0.2399 | 0.2186 | 0.2381 | 37.07 | 25.23 | 20.27 |
| Average of Ga | 0.0005 | 0.0004 | 0.0004 | Average of Ga | 0.0026 | 0.0018 | 0.0030 | 0.0024 | 81.96 | 77.41 | 85.87 |
| Average of As | 0.0042 | 0.0046 | 0.0055 | Average of As | 0.0043 | 0.0053 | 0.0063 | 0.0084 | 2.43 | 12.67 | 13.16 |
| Average of Se | 0.0020 | 0.0021 | 0.0022 | Average of Se | 0.0004 | 0.0003 | 0.0004 | 0.0005 | -367.48 | -491.22 | -465.74 |
| Average of Br | 0.0121 | 0.0129 | 0.0127 | Average of Br | 0.0108 | 0.0106 | 0.0099 | 0.0116 | -11.43 | -22.39 | -27.64 |
| Average of Rb | 0.0032 | 0.0036 | 0.0043 | Average of Rb | 0.0019 | 0.0020 | 0.0025 | 0.0029 | -69.19 | -80.36 | -69.05 |
| Average of Sr | 0.0011 | 0.0013 | 0.0011 | Average of Sr | 0.0015 | 0.0011 | 0.0011 | 0.0015 | 21.32 | -13.64 | -4.53 |
| Average of Y | 0.0002 | 0.0001 | 0.0001 | Average of Y | 0.0003 | 0.0004 | 0.0004 | 0.0004 | 50.60 | 87.55 | 67.91 |
| Average of Zr | 0.0005 | 0.0006 | 0.0006 | Average of Zr | 0.0010 | 0.0016 | 0.0013 | 0.0007 | 48.14 | 62.20 | 55.02 |
| Average of Mo | 0.0007 | 0.0005 | 0.0005 | Average of Mo | 0.0012 | 0.0015 | 0.0011 | 0.0017 | 42.70 | 63.41 | 51.13 |
| Average of Pd | 0.0011 | 0.0012 | 0.0017 | Average of Pd | 0.0020 | 0.0019 | 0.0014 | 0.0016 | 41.94 | 35.98 | -23.74 |
| Average of Ag | 0.0014 | 0.0011 | 0.0017 | Average of Ag | 0.0012 | 0.0013 | 0.0020 | 0.0018 | -24.21 | 20.55 | 16.39 |
| Average of Cd | 0.0022 | 0.0019 | 0.0023 | Average of Cd | 0.0018 | 0.0022 | 0.0021 | 0.0025 | -24.37 | 13.60 | -8.17 |
| Average of In | 0.0014 | 0.0018 | 0.0020 | Average of In | 0.0011 | 0.0009 | 0.0010 | 0.0017 | -23.61 | -102.47 | -104.22 |
| Average of Sn | 0.0116 | 0.0188 | 0.0203 | Average of Sn | 0.0084 | 0.0131 | 0.0118 | 0.0162 | -38.68 | -43.34 | -72.14 |
| Average of Sb | 0.0038 | 0.0046 | 0.0049 | Average of Sb | 0.0033 | 0.0042 | 0.0027 | 0.0039 | -12.96 | -10.29 | -83.27 |
| Average of Ba | 0.0089 | 0.0267 | 0.0170 | Average of Ba | 0.0053 | 0.0106 | 0.0081 | 0.0068 | -69.41 | -151.71 | -108.29 |
| Average of La | 0.0130 | 0.0131 | 0.0087 | Average of La | 0.0112 | 0.0105 | 0.0081 | 0.0082 | -15.97 | -24.15 | -7.76 |
| Average of Au | 0.0004 | 0.0003 | 0.0005 | Average of Au | 0.0003 | 0.0003 | 0.0006 | 0.0002 | -59.90 | -6.51 | 28.70 |
| Average of Hg | 0.0001 | 0.0001 | 0.0002 | Average of Hg | 0.0001 | 0.0000 | 0.0003 | 0.0001 | -6.72 | -142.43 | 42.22 |
| Average of Tl | 0.0001 | 0.0001 | 0.0001 | Average of Tl | 0.0003 | 0.0002 | 0.0001 | 0.0000 | 54.88 | 58.44 | -41.75 |
| Average of Pb | 0.0576 | 0.0664 | 0.0726 | Average of Pb | 0.0432 | 0.0478 | 0.0498 | 0.0624 | -33.38 | -38.97 | -45.80 |
| Average of U | 0.0002 | 0.0002 | 0.0002 | Average of U | 0.0018 | 0.0013 | 0.0011 | 0.0017 | 91.64 | 83.60 | 83.62 |

# 5. SUMMARY AND RECOMMENDATIONS

Between 11/3/2004 and 10/29/2005, chemically speciated $PM_{2.5}$ was measured every sixth day in Hong Kong at four sites representing air quality at roadside, urban, and rural areas. A total of 61 samples were collected from the Mong Kok (MK), Tsuen Wan (TW), Yuen Long (YL), and Hok Tsui (HT) sites. The highest annual mean $PM_{2.5}$ mass of ~53 μg $m^{-3}$ was found at the roadside MK site. The lowest annual mean of ~28 μg $m^{-3}$ was found at the rural HT site, but this value is still much higher than the USEPA annual 24-hr $PM_{2.5}$ standard of 15 μg $m^{-3}$.

Data was validated through various comparisons between measurements. Reconstructed mass and measured mass were highly correlated with $r^2 \sim 0.99$, which further confirmed the validity of gravimetric and chemical measurements. Carbonaceous aerosol accounted for more than half of $PM_{2.5}$ mass at MK. The EC/OC ratio of almost 1 at the roadside MK site indicated the substantial influence of motor-vehicle exhaust. Sulfate contributed equally at the TW and YL sites (42 %) and was higher at the HT site (54%) and lowest at the MK site (31%). Nitrate was significantly lower at all four sites. Ammonium was well balanced by sulfate and nitrate at all four sites. Concentrations of crustal material and trace elements were low, accounting for <15 % of $PM_{2.5}$ mass and lacking distinct spatial variations.

High sulfate concentrations did not necessarily appear in summer. The two highest sulfate episodes appeared on 9/11/05 and 10/17/05. Sulfate concentrations were similar at all three sites, suggesting that sulfate and its gaseous precursor ($SO_2$) may have originated from more distant upwind sources. Even though wind directions varied from winter to summer due to Asian monsoons, seasonal variations in sulfate concentrations were not clear. Measurements are needed over several years to establish a statistically significant seasonal and interannual variation.

EC concentrations at MK were generally higher than at the other three sites, but no significant seasonal trend was observed. OC at MK was generally higher in winter, which led to a lower EC/OC ratio in winter. Whether this is due to aerosol microphysics or atmospheric boundary-layer dynamics warrants further investigation. A close comparison of EC concentrations with local meteorological parameters, such as wind speed, wind direction, and boundary-layer mixing height should provide useful insights.

Crustal material concentrations at all four sites were also similar and may be attributable to long-range transport of fine-mode fugitive dust. There were a few extremely high dust events, including one episode that occurred on 11/3/04. At HT, the dust events tracked the EC concentration rather well, and therefore road dust from traffic in the nearby urban areas might also be important. Further data analysis needs to examine the variation of dust composition, such as the Si/Ca ratio to identify the most likely origins.

Variation of PM2.5 mass concentrations and their major components over sites and years are also evaluated. The reduction in $PM_{2.5}$ mass and carbon levels at MK indicates an effective control of vehicular emissions over the years which significantly reduce the roadside carbon as well as $PM_{2.5}$ levels. With regard to the variation of secondary pollutants (sulfate, nitrate and ammonium) which are often considered as markers for regional

pollutants, a substantial growth is identified at all the sites. The result reveals that Hong Kong has been adversely affected by the increasing impact of regional pollution.

Recommendations for future work include:

1. Long-term monitoring: The USEPA requires three years of monitoring to determine compliance with standards. This is to compensate for potential abnormalities in climate patterns that may significantly influence pollution levels. Long-term monitoring also helps to determine seasonal and interannual trends.

2. Source quantification: This study acquired rich inorganic and organic ambient data. However, better knowledge of local and regional pollution sources is needed in order to understand how emissions are related to ambient concentrations, human exposure, and health effects. Such knowledge can be obtained by measuring source emissions, determining emission profiles, and estimating emission inventories. Similar data from other countries are not necessarily applicable to Hong Kong because of differences in sources and atmospheric transformation.

3. Data analysis: A comprehensive data analysis effort that integrates meteorological and chemical data is very important to implementing effective pollution controls and regulations. This may include chemical mass balance analysis (which requires source information) and factor analysis to quantify contributions from all potential sources. Receptor models, such as wind rose and ensemble air parcel back trajectory, are useful for determining source regions and providing a basis for full chemical transport modeling.

## 6. REFERENCES


Bevington, P.R. (1969). *Data Reduction and Error Analysis for the Physical Sciences.* McGraw Hill, New York, NY.

Chen, L.-W.A.; Chow, J.C.; Watson, J.G.; Moosmüller, H.; and Arnott, W.P. (2004). Modeling reflectance and transmittance of quartz-fiber filter samples containing elemental carbon particles: Implications for thermal/optical analysis. *J. Aerosol Sci.*, **35**(6):765-780.

Chow, J.C. (1995). Critical review: Measurement methods to determine compliance with ambient air quality standards for suspended particles. *J. Air Waste Manage. Assoc.*, **45**(5):320-382.

Chow, J.C.; and Watson, J.G. (1989). Summary of particulate data bases for receptor modeling in the United States. In *Transactions, Receptor Models in Air Resources Management*, J.G. Watson, Ed. Air & Waste Management Association, Pittsburgh, PA, pp. 108-133.

Chow, J.C.; and Watson, J.G. (1992). Fugitive emissions add to air pollution. *Environ. Protect.*, **3**:26-31.

Chow, J.C.; and Watson, J.G. (1994). Contemporary source profiles for geological material and motor vehicle emissions. Report No. DRI 2625.2F. Prepared for U.S. EPA, Office of Air Quality Planning and Standards, Research Triangle Park, NC, by Desert Research Institute, Reno, NV.

Chow, J.C.; and Watson, J.G. (1999). Ion chromatography in elemental analysis of airborne particles. In *Elemental Analysis of Airborne Particles, Vol. 1*, S. Landsberger and M. Creatchman, Eds. Gordon and Breach Science, Amsterdam, pp. 97-137.

Chow, J.C.; Watson, J.G.; Chen, L.-W.A.; Arnott, W.P.; Moosmüller, H.; and Fung, K.K. (2004). Equivalence of elemental carbon by Thermal/Optical Reflectance and Transmittance with different temperature protocols. *Environ. Sci. Technol.*, **38**(16):4414-4422.

Chow, J.C.; Watson, J.G.; Crow, D.; Lowenthal, D.H.; and Merrifield, T.M. (2001). Comparison of IMPROVE and NIOSH carbon measurements. *Aerosol Sci. Technol.*, **34**(1):23-34.

Chow, J.C.; Watson, J.G.; Lowenthal, D.H.; Solomon, P.A.; Magliano, K.L.; Ziman, S.D.; and Richards, L.W. (1993a). $PM_{10}$ and $PM_{2.5}$ compositions in California's San Joaquin Valley. *Aerosol Sci. Technol.*, **18**:105-128.

Chow, J.C.; Watson, J.G.; Lu, Z.; Lowenthal, D.H.; Frazier, C.A.; Solomon, P.A.; Thuillier, R.H.; and Magliano, K.L. (1996). Descriptive analysis of $PM_{2.5}$ and $PM_{10}$ at regionally representative locations during SJVAQS/AUSPEX. *Atmos. Environ.*, **30**(12):2079-2112.

Chow, J.C.; Watson, J.G.; Pritchett, L.C.; Pierson, W.R.; Frazier, C.A.; and Purcell, R.G. (1993b). The DRI Thermal/Optical Reflectance carbon analysis system: Description, evaluation and applications in U.S. air quality studies. *Atmos. Environ.*, **27A**(8):1185-1201.

Fitz, D.R. (1990). Reduction of the positive organic artifact on quartz filters. *Aerosol Sci. Technol.*, **12**(1):142-148.

Green, M.C.; Chow, J.C.; Hecobian, A.; Etyemezian, V.; Kuhns, H.D.; and Watson, J.G. (2002). Las Vegas Valley Visibility and $PM_{2.5}$ Study: Final report. Prepared for Clark County Dept. of Air Quality Management, Las Vegas, NV, by Desert Research Institute, Las Vegas, NV.

Hidy, G.M. (1985). Jekyll Island meeting report: George Hidy reports on the acquisition of reliable atmospheric data. *Environ. Sci. Technol.*, **19**(11):1032-1033.

Lee, K.W.; and Ramamurthi, M. (1993). Filter collection. In *Aerosol Measurement: Principles, Techniques and Applications*, K. Willeke and P.A. Baron, Eds. Van Nostrand, Reinhold, New York, NY, pp. 179-205.

Lioy, P.J.; Watson, J.G.; and Spengler, J.D. (1980). APCA specialty conference workshop on baseline data for inhalable particulate matter. *J. Air Poll. Control Assoc.*, **30**(10):1126-1130.

Lippmann, M. (1989). Sampling aerosols by filtration. In *Air Sampling Instruments for Evaluation of Atmospheric Contaminants*, 7 ed., S.V. Hering, Ed. American Conference of Governmental Industrial Hygienists, Cincinnati, OH, pp. 305-336.

Louie, P.K.K.; Chow, J.C.; Chen, L.-W.A.; Watson, J.G.; Leung, G.; and Sin, D. (2005a). PM2.5 chemical composition in Hong Kong: Urban and regional variations. *Sci. Total Environ.*, **338**(3):267-281.

Louie, P.K.K.; Watson, J.G.; Chow, J.C.; Chen, L.-W.A.; Sin, D.W.M.; and Lau, A.K.H. (2005b). Seasonal characteristics and regional transport of PM2.5 in Hong Kong. *Atmos. Environ.*, **39**(9):1695-1710.

Turpin, B.J.; Huntzicker, J.J.; and Hering, S.V. (1994). Investigation of organic aerosol sampling artifacts in the Los Angeles Basin. *Atmos. Environ.*, **28**(19):3061-3071.

Watson, J.G.; and Chow, J.C. (1993). Ambient air sampling. In *Aerosol Measurement: Principles, Techniques and Applications*, K. Willeke and P.A. Baron, Eds. Van Nostrand, Reinhold, New York, NY, pp. 622-639.

Watson, J.G.; and Chow, J.C. (1994). Particle and gas measurements on filters. In *Environmental Sampling for Trace Analysis*, B. Markert, Ed. VCH, New York, pp. 125-161.

Watson, J.G.; Chow, J.C.; and Frazier, C.A. (1999). X-ray fluorescence analysis of ambient air samples. In *Elemental Analysis of Airborne Particles, Vol. 1*, S. Landsberger and M. Creatchman, Eds. Gordon and Breach Science, Amsterdam, pp. 67-96.

Watson, J.G.; Chow, J.C.; Lowenthal, D.H.; Pritchett, L.C.; Frazier, C.A.; Neuroth, G.R.; and Robbins, R. (1994). Differences in the carbon composition of source profiles for diesel- and gasoline-powered vehicles. *Atmos. Environ.*, **28**(15):2493-2505.

Watson, J.G.; Lioy, P.J.; and Mueller, P.K. (1989). The measurement process: Precision, accuracy, and validity. In *Air Sampling Instruments for Evaluation of Atmospheric Contaminants, Seventh Edition,* 7th ed., S.V. Hering, Ed. American Conference of Governmental Industrial Hygienists, Cincinnati, OH, pp. 51-57.

Watson, J.G.; Turpin, B.J.; and Chow, J.C. (2001). The measurement process: Precision, accuracy, and validity. In *Air Sampling Instruments for Evaluation of Atmospheric Contaminants, Ninth Edition,* 9th ed., B.S. Cohen and C.S.J. McCammon, Eds. American Conference of Governmental Industrial Hygienists, Cincinnati, OH, pp. 201-216.